

WEDISSON OLIVEIRA SANTOS

**PRODUÇÃO DE FERTILIZANTES POTÁSSICOS E FOSFATADOS POR MEIO
DE PROCESSOS TÉRMICOS E QUÍMICOS E AVALIAÇÃO DA EFICIÊNCIA
AGRONÔMICA**

Tese apresentada à Universidade Federal de Viçosa,
como parte das exigências do Programa de Pós-
Graduação em Solos e Nutrição de Plantas, para
obtenção do título de *Doctor Scientiae*.

VIÇOSA
MINAS GERAIS – BRASIL
2015

**Ficha catalográfica preparada pela Biblioteca Central da Universidade
Federal de Viçosa - Câmpus Viçosa**

T

Santos, Wedisson Oliveira, 1981-
S237p Produção de fertilizantes potássicos e fosfatados por meio
2015 de processos térmicos e químicos e avaliação da eficiência
 agronômica / Wedisson Oliveira Santos. – Viçosa, MG, 2015.
 ix, 72f. : il. (algumas color.) ; 29 cm.

Orientador: Edson Marcio Mattiello.
Tese (doutorado) - Universidade Federal de Viçosa.
Inclui bibliografia.

1. Adubos e fertilizantes. 2. Fosfatos. 3. Fertilizantes
potássicos. 4. Fertilizantes fosfatados. I. Universidade Federal
de Viçosa. Departamento de Solos. Programa de Pós-graduação
em Solos e Nutrição de Plantas. II. Título.

CDD 22. ed. 631.8

WEDISSON OLIVEIRA SANTOS

**PRODUÇÃO DE FERTILIZANTES POTÁSSICOS E FOSFATADOS POR MEIO
DE PROCESSOS TÉRMICOS E QUÍMICOS E AVALIAÇÃO DA EFICIÊNCIA
AGRONÔMICA**

Tese apresentada à Universidade Federal de Viçosa,
como parte das exigências do Programa de Pós-
Graduação em Solos e Nutrição de Plantas, para
obtenção do título de *Doctor Scientiae*.

APROVADA: 10 de dezembro de 2015

Ivo Ribeiro da Silva

Carlos Ernesto Gonçalves Reynaud Schaefer

Guilherme Lopes

Luiz Francisco da Silva Souza Filho

Edson Marcio Mattiello
(Orientador)

Aos meus pais, *Anália* e *Salviano*, pelo exemplo de dignidade, confiança e apoio.

À minha esposa *Carolina*, pelo amor e incentivo.

Aos meus irmãos *Willas*, *Wellis* e *Heila*.

Às cunhadas *Rafaella* e *Bettina*.

Aos meus sogros *José Roberto* e *Grasiela*.

Dedico

“A mente que se abre para algo novo, nunca mais será a mesma”.

(Albert Einstein)

AGRADECIMENTOS

Em primeiro lugar, à Deus, por tudo.

À Universidade Federal de Viçosa, por meio do Departamento de Solos, por possibilitar a realização deste curso.

À CAPES, FAPEMIG e CNPq, pelos auxílios financeiros.

À North Carolina State University por possibilitar o “*sandwich doctorate*”.

Ao Professor Edson Marcio Mattiello, pela orientação e amizade.

Ao Professor Dean Hesterberg, pelos ensinamentos e amizade.

Ao Professor Leonardus Vergutz, pela co-orientação e amizade.

Aos demais Professores do DPS, por contribuírem com a minha formação, destacando Victor Hugo Alvarez V, Roberto Ferreira de Novais, João Carlos Ker, Edson Marcio Mattiello, Liovando Marciano da Costa, Rafael Bragança, Maurício Fontes, Ivo Ribeiro da Silva, Emanuelle Mercês Barros Soares, Júlio César Lima Neves e Reinaldo Bertola Cantarutti .

Aos Funcionários do Departamento de Solos e Pós-graduação, especialmente Paulo, Mario, Chico da Mineralogia, Carlos Fonseca, Cláudio, Luiz Fernando, Jorge Orlando, Geraldo Robésio, Luciana e Leiliane.

À Rúbio Rodrigues, Laura Guimarães, Rodolfo Fagundes, Rafael Lucas Coca Cuesta, Gabriella Braga Rocha e Patrícia Cardoso Matias, pelas valiosas contribuições na execução dos experimentos.

Aos colegas da Pós-graduação, especialmente Nicolás Ignacio Stahringer, Odirley Rodrigues Campos, Patrícia Cardoso Matias, Fernanda Schulthais, Aline Vasconcellos, Gabriel Reis, Ivan Francisco, Gelton, Diogo Paiva, Evair, Gustavo, Guilherme, Cristiano, Matheus Baiano, Jeferson Paes, Bárbara Elias Reis, Anderson Pacheco, Silmara, Luiz Felipe Mesquita, Júlia Gomes Ferreira, Samuel e Rafael Valadares, pela amizade.

BIOGRAFIA

WEDISSON OLIVEIRA SANTOS, filho de Salviano Cândido dos Santos e Anália Oliveira Santos, nasceu em 9 de janeiro de 1981, em Andaraí- BA.

Em dezembro de 1999, concluiu o curso de Técnico em Agronomia pela Escola Agrotécnica Federal de Catu (EAFC), atual Instituto Federal de Educação da Bahia (IFBA).

Em maio de 2000, ingressou na Fazenda Progresso como Técnico Agrícola na área de Olericultura, até agosto de 2005.

Em agosto de 2005, iniciou a graduação em Engenharia Agrônômica pela Universidade Estadual do Sudoeste da Bahia (UESB), concluindo-o em agosto de 2010.

Em agosto de 2010, iniciou o mestrado em Solos e Nutrição de Plantas na Universidade Federal de Viçosa (UFV), sob orientação do Professor Edson Marcio Mattiello, concluindo-o em fevereiro de 2012.

Em fevereiro de 2012, iniciou o doutorado em Solos e Nutrição de Plantas na UFV, sob orientação do Professor Edson Marcio Mattiello, concluindo-o em dezembro de 2015.

Entre março de 2014 e fevereiro de 2015, realizou “*sandwich doctorate*”, através do programa Ciências sem Fronteiras, na North Carolina State University (NCSU), sob orientação do Professor Dean Hesterberg.

SUMÁRIO

RESUMO	vi
ABSTRACT	viii
INTRODUÇÃO GERAL	1
ARTIGO 1	4
Thermal treatment of a potassium-rich metamorphic rock in formation of soluble K forms	4
ARTIGO 2	23
Increasing soluble phosphate species by treatment of phosphate rocks with acidic mine waste	23
ARTIGO 3	48
Production and evaluation of potassium fertilizers from silicate rock	48
CONCLUSÕES GERAIS	72

RESUMO

SANTOS, Wedisson Oliveira, D.Sc., Universidade Federal de Viçosa, dezembro de 2015. **Produção de fertilizantes potássicos e fosfatados por meio de processos térmicos e químicos e avaliação da eficiência agrônômica.** Orientador: Edson Marcio Mattiello. Coorientador: Leonardus Vergutz.

A presente tese trata-se de estudos relacionados ao desenvolvimento de fertilizantes utilizando processos térmicos e químicos, e avaliações agrônômicas. Para o trabalho 1, uma rocha silicatada potássica, chamada verdete (RV) foi calcinada na presença e ausência de um agente fundente (AF), o $\text{CaCl}_2 \cdot 2\text{H}_2\text{O}$, variando a temperatura de calcinação e proporção (m m^{-1}) AF/RV, objetivando a produção de um fertilizante potássico solúvel. Foram medidos os teores de K solúveis em água e investigadas transformações minerais por meio de difração de raios X (DRX) ou do ambiente molecular do K, por meio de espectroscopia de absorção de raios X (XAS). Demonstrou-se que a RV tem baixa solubilidade em água, entretanto quando calcinada em condições ótimas de temperatura (850 °C) e proporção (m m^{-1}) AF/RV (1.7) é possível extrair em água até 95% (m m^{-1}) do K total da rocha. De acordo com a análise de Potassium K-edge XANES, a formação de silicato de potássio de baixa cristalinidade (*bc*- K_2SiO_3) é linear positiva com o aumento da temperatura até 1100 °C, já a formação de KCl é otimizada a 850 °C. Os teores de K extraídos em água diminuíram de 900 para 1100 °C, e a análise Linear Combination Fitting analysis (LCF) indicou diminuição da espécie KCl (elevada solubilidade) e aumento da proporção de *bc*- K_2SiO_3 (baixa solubilidade), sugerindo a conversão de formas solúveis de K em fases vítreas de baixa solubilidade. Elevados resíduos da análise LCF, de até 0,04, indicam a formação de desconhecidas espécies de K, que não foram utilizadas como padrões para essa análise. Para o segundo trabalho, fosfatos naturais oriundos de Patos, Araxá e do Perú (Bayóvar) reagiram com diferentes concentrações de efluente ácido (EA). Teores solúveis de P em água, ácido cítrico e em citrato neutro de amônio, comprovaram o aumento da solubilização desses fosfatos com o aumento da concentração de EA. Entretanto, para o fosfato de Patos, ajustes quadráticos

revelaram que o EA promoveu maior extração de P em concentrações entre 40 e 60% (v v⁻¹). Análises de Phosphorus K-edge XANES e DRX mostraram que ao longo da dissolução da apatita, com o aumento da concentração do EA, ocorre formação de sulfatos de cálcio (DRX) e espécies de P mais solúveis (XANES), como fosfato tricálcico amorfo, fosfato dicálcico, fosfato monocálcio e fosfato de ferro amorfo. Análise na pré-borda do P (~2148 eV) mostra que a formação de fosfatos de ferro (III) é progressiva com o aumento da concentração do efluente. Adicionalmente, a suavização da pós-edge (~ 2155 eV) com o aumento da concentração do efluente, confirma a formação de espécies de P menos rica em Ca. Para o trabalho 3, foram produzidos fertilizantes potássicos por meio de calcinação e ataque ácido da RV, utilizando cloreto de cálcio como AF e o EA de indústria metalúrgica, respectivamente. Caracterizações mineralógicas da RV calcinada (VC) e acidificada (VA) confirmaram a formação de minerais potássicos solúveis, a sylvita (KCl) e a arcanita (K₂SO₄), respectivamente. Foram realizados ensaios em casa de vegetação utilizando milho (*Zea mays* L.), capim (*Panicum maximum* cv. Mombaça), e eucalipto (clone I144) como plantas teste. Como fontes de K, utilizou-se a RV, VC, VA e o KCl. A RV mostrou-se ser pouco reativa, com insignificante efeito nos cultivos de milho e eucalipto. Entretanto, pequeno efeito residual foi observado no cultivo de capim, subsequente ao milho. De forma geral, as performances do VC e VA em termos de absorção de K pelo milho, capim e eucalipto foram equivalentes ou superiores ao KCl. Os resultados obtidos com essa tese mostram que é possível obter fertilizante potássico com eficiência agrônômica equiparável ao KCl, a partir do reaproveitamento de um resíduo e exploração de uma rocha silicatada. A calcinação mostrou-se mais eficaz que a acidificação da RV, entretanto estudos de viabilidade econômica com tais processos são necessários. A reutilização do EA na solubilização de fosfatos naturais parece ser promissora, diante do expressivo aumento de reatividade dos fosfatos de Araxá, Patos e Bayóvar alcançados com a acidificação. Entretanto, estudos com plantas são necessários para a comprovação da eficácia desses produtos como fertilizantes.

ABSTRACT

SANTOS, Wedisson Oliveira, D.Sc., Universidade Federal de Viçosa, December, 2015. **Production of potassium and phosphate fertilizers by thermal and chemical processes and evaluation of agronomic efficiency.** Adviser: Edson Marcio Mattiello. Co-adviser: Leonardus Vergutz.

This thesis presents studies related to development of potassium and phosphate fertilizers using thermal and chemical processes, and agronomic evaluations. For work 1, a potassium silicate-rock, called verdete (VR), was calcined in presence and absence of a melting agent (MA), $\text{CaCl}_2 \cdot 2\text{H}_2\text{O}$, considering different calcination temperatures and MA/VR ratios (w w^{-1}), aiming to produce a soluble potassium fertilizer. It were measured soluble K contents in water and also was investigated mineral transformations, by X ray diffraction (XRD) or changes in K molecular environment, through X ray absorption spectroscopy (XAS). VR has low water solubility, however when it was calcined in optimal conditions of temperature ($850\text{ }^\circ\text{C}$) and MA/VR ratio (1.7 w w^{-1}) was possible to extract in water 95% of total K. According to Potassium K-edge XANES analysis, the formation of potassium silicate low crystalline (*lc*- K_2SiO_3) increases over temperature calcination until $1100\text{ }^\circ\text{C}$, already KCl formation, is optimized at $850\text{ }^\circ\text{C}$. Amounts of extracted K in water (K_{water}) decreased from $900\text{ }^\circ\text{C}$ to $1100\text{ }^\circ\text{C}$, when Linear Combination Fitting analysis (LCF) indicated decreasing of KCl specie (high solubility) and increase of *lc*- K_2SiO_3 (low solubility), suggesting the conversion of soluble K phases into low soluble vitreous K phases. High residues of LCF, until 0.04, suggest the presence of unknown K species, which were not used as standards to perform this analysis. In second work, phosphate rocks (PRs) from Patos and Araxá (Brazil) and Bayóvar (Peru) reacted with different concentrations of an acidic mining waste (AMW) from a metallurgic industry. Extractable P in water, citric acid and in neutral ammonium citrate confirmed the increasing of solubilization of these PRs, over increasing AMW concentration. However, for Patos PR, quadratic fits revealed that AMW promoted optimal P solubilization between 40 and 60% (v v^{-1}). Phosphorus K-edge XANES analysis showed

that following apatite dissolution, increasing AMW concentration, calcium sulfates were formed (detected by XRD), as well as more soluble P species (detected by XANES), like amorphous tricalcium phosphate, dicalcium phosphate, monocalcium phosphate and amorphous iron (III) phosphate. Analysis in P pre-edge (~2148 eV) reveal that formation of iron (III) phosphate is progressive with increasing AMW concentration. Additionally, mitigation of post-edge shoulder (~2155 eV) with increasing AMW concentration, confirms formation of P species less rich in Ca. For work 3, we produced potassium fertilizers by calcination (CV) and acid attack in VR (AV), using calcium chloride as MA and the AMW, respectively. Mineralogical characterization of VR, CV and AV, confirmed the formation of soluble K minerals, as sylvite (KCl) and arcanite (K₂SO₄), respectively. Greenhouse trials were carried out in protected environment (greenhouse) using maize (*Zea mays* L.), grass (*Panicum maximum* cv. Mombaça) and eucalyptus (I144 clone) as test plants. Like K sources, we used VR, CV, AV and KCl. VR showed to be little reactive, demonstrating insignificant effect to maize or eucalyptus growth. However, small residual effect was observed to grass crop (successive cultivation after maize). Overall, VC and AV performances, in terms of K uptake by maize and eucalyptus, were equivalent or higher than KCl. Results obtained with this thesis show that is possible to get potassium fertilizers with agronomic efficiency equiparable with KCl, reusing an acidic waste and exploring a silicate rock. Calcination treatment showed to be more efficient than acidification of VR, however economic viability studies with such processes are necessary. Reusing of AMW to solubilize PR looks promising, because of expressive increasing of reactivity of Araxá, Patos e Bayóvar RPs by their acidification. However, studies with plants are necessary to confirm efficacy of these products as fertilizers.

INTRODUÇÃO GERAL

O Brasil é um país com amplas possibilidades de se tornar uma referência mundial para atendimento da crescente demanda por alimentos, madeira, fibras e energia, decorrentes do crescimento populacional. Além de possuir grande disponibilidade de áreas agricultáveis, os principais cultivos agrícolas no país ainda apresentam plenas condições de aumentos expressivos de produtividade. Entretanto, políticas agrícolas ineficientes, problemas com logística de produção e transporte, insuficiência na conservação dos solos, e à baixa fertilidade dos solos, representam desafios para o agronegócio brasileiro.

A baixa fertilidade dos solos agricultados brasileiros resulta na necessidade de aplicação de doses elevadas de fertilizantes para obtenção de produtividades viáveis. No entanto, o país é dependente de fornecimento externo de fertilizantes. Apenas cerca de 25% dos fertilizantes utilizados na agricultura brasileira são provenientes da produção doméstica. Entre os nutrientes, a situação mais crítica é a do K. O país importa mais de 90% dos fertilizantes potássicos consumidos e não possui perspectiva de ampliação de suas reservas no longo prazo (Lima & Neves, 2014). Por outro lado, é grande a ocorrência de minerais silicatados ricos em K no Brasil, entretanto a baixa solubilidade desses materiais inviabilizam seus usos *in natura*, havendo necessidade de estudos para viabilizar o uso dessas fontes na produção de fertilizantes.

O Brasil também apresenta grande dependência externa de fertilizantes fosfatados, importando cerca de 50% do total utilizados na agricultura (Lima & Neves, 2014). Os fosfatos brasileiros por apresentarem baixa qualidade agronômica, devido à suas origens ígneas, grau de metamorfismo dos depósitos ou a baixa substituição isomórfica de PO_4^{3-} por CO_3^{2-} nas estruturas apatíticas, necessitam de solubilização parcial ou total em meio ácido ou tratamentos térmicos para uso como fertilizantes. Geralmente se utiliza o ácido sulfúrico ou fosfórico para solubilizar esses fosfatos, representando expressiva participação no custo de produção desses insumos (Beisiegel & Souza, 1986; Oba, 2004; Prochnow et al. 2004; Lapido-Loureiro & Melamed, 2006; Faria & Guardieiro, 2011). Por outro lado, atividades metalúrgicas que utilizam digestão ácida de minérios, geram grande quantidades de resíduos com elevada acidez. Tais resíduos são impróprios para o descarte no ambiente e por isso são

neutralizados e estocados, implicando em elevado custo com esses tratamentos. O reaproveitamento desses materiais para a produção de fertilizantes é oportuno, podendo implicar em menor custo de produção desses insumos, além do benefício ambiental. Por se tratarem de misturas ácidas, contendo em muitos casos o ácido fluorídrico, esses resíduos são potenciais para solubilizar além de fosfatos naturais, minerais silicatados potássicos.

Para caracterização de materiais, amostras de solo, produtos das reações, incluindo fertilizantes, o ideal é o uso de várias técnicas, de forma complementares. O conhecimento dos teores solúveis dos nutrientes nos fertilizantes é essencial para inferir sobre a reatividade do material e a biodisponibilidade dos nutrientes, entretanto não informa sobre as espécies formadas. Nesse sentido, a difração de raios X (DRX) é a técnica mais utilizada na identificação de minerais, mas se limita às formas cristalinas. Por outro lado, técnicas baseadas em luz síncrotron, como absorção de raios X (XAS) surgem como alternativas complementar para a identificação de fases, independentemente do grau de organização estrutural (Kelly et al., 2008).

A partir da década de 1980, o surgimento de laboratórios de luz síncrotron permitiram o armazenamento de elétrons de alta energia ($E \geq 1\text{GeV}$), tornando possível a obtenção de espectros com boa relação sinal/ruído, viabilizando a expansão de estudos no campo da espectroscopia de absorção de raios X no mundo (Mazali, 1998; Kelly et al., 2008). Apesar da grande evolução na utilização dessa técnica nas últimas décadas, no ramo das ciências agrárias no Brasil sua utilização ainda é muito incipiente.

A absorção de raios X se dá por meio de transições eletrônicas, geralmente nos subníveis quânticos 1s ou 2p, sendo que o espectro de absorção de raios X representa a média ponderada dos ambientes de coordenação molecular do elemento absorvedor. Nesses espectros, duas regiões se definem, a XANES e EXAFS, que envolvem princípios físicos diferentes. A região de XANES (X-ray absorption near edge structure), compreendida entre -50 e +200 eV relativo a energia da borda de absorção (E_0), apresenta intensas variações no coeficiente de absorção. O comprimento de ondas de fotoelétrons nessa região é da ordem de distâncias interatômicas, envolvendo espalhamentos múltiplos e transições eletrônicas para níveis desocupados, permitindo a obtenção de informações sobre o estado de oxidação do átomo absorvedor e sobre a composição de sistemas contendo diferentes fases do elemento. Já a região EXAFS (Extended X-ray absorption fine structure), corresponde a

absorção de energia acima da região XANES até em torno de +1000 eV acima de E_0 . Nessa região ocorre o espalhamento simples de radiação envolvendo o átomo absorvedor e espalhadores. O caminho livre médio do fotoelétron nessa região é curto, permitindo modelar sobre o número e distância média dos átomos vizinhos em relação ao absorvedor nas primeiras esferas de coordenação, assim como o grau de desordem estrutural (Kelly et al., 2008).

Faça ao exposto, a presente tese, com o título genérico “*PRODUÇÃO DE FERTILIZANTES POTÁSSICOS E FOSFATADOS POR MEIO DE PROCESSOS TÉRMICOS E QUÍMICOS E AVALIAÇÃO DA EFICIÊNCIA AGRONÔMICA*” propôs investigações da extractabilidade de K e P de amostras de verdete ou fosfatos naturais submetidas a tratamento térmico ou químico, respectivamente. Transformações minerais foram estudadas por meio de DRX e do ambiente molecular do K e P, por XANES. Ensaio agronômicos foram realizados objetivando avaliar a eficiência de fertilizantes potássicos produzidos por ataque ácido ou calcinação.

REFERÊNCIAS

- Beisiegel WR, Souza WO (1986) Reservas de fosfatos--Panorama nacional e mundial. Instituto Brasileiro de Fosfato (IBRAFOS) III Encontro Nacional de Rocha Fosfática, Brasília, 16.
- Faria FM, Guardieiro GA (2011) Adubação fosfatada na cultura da soja. Revista Passarela da Soja 1, 105-111.
- Kelly SD, Hesterberg D, Ravel B (2008) Analysis of soils and minerals using X-ray absorption spectroscopy. Methods of soil analysis Part 5:387-463
- Lapido-Loureiro FEV, Melamed R (2006) O fósforo na agricultura brasileira: uma abordagem minero-metalúrgica. Centro de Tecnologia Mineral: Rio de Janeiro.
- Lima TM, Neves CAR (2012). Sumário Mineral 2014. In Departamento Nacional de Produção Mineral, DNPM. DNPM: Brasília, 141.
- Mazali IO (1998). "EXAFS como técnica de caracterização estrutural de materias: Fundamentos Teóricos e Aplicações." LQES - Laboratório de Química do Estado Sólido – Instituto de Química – UNICAMP. Disponível em: <http://lqes.iqm.unicamp.br/>. Acessado em: 15 dez 2015.
- Oba, CAI (2004) Fabricação de um fertilizante organo-fosfatado. Rio de Janeiro: CETEM/MCT.
- Prochnow LI, Chien SH, Carmona G, Henao J (2004). Greenhouse evaluation of phosphorus sources produced from a low-reactive Brazilian phosphate rock. Agron J 96, 761-768.

ARTIGO 1

Thermal treatment of a potassium-rich metamorphic rock in formation of soluble K forms

Wedisson Oliveira Santos^{1*}, Edson Marcio Mattiello¹, Anderson Almeida Pacheco¹, Leonardus Vergutz¹, Luiz Francisco da Silva Souza-Filho¹, Dalton Belchior Abdala²

¹Departament of Soil Science, Universidade Federal de Viçosa, Viçosa, Minas Gerais, Brazil;

² Brazilian Synchrotron Light Laboratory – LNLS, Campinas, São Paulo - Brazil

Abstract

Countries like Brazil, China and India have high external dependence and limited reserves of soluble potassium minerals, not yet traditionally exploited for the production of fertilizers. Thus, the common occurrence of potassium-rich silicate minerals in these countries, not yet commercially exploited, have stimulated the search for new ways on how increase the reactivity of these minerals and to use them as a raw material to produce fertilizers. This work aimed to investigate the calcination of a potassium rock (verdete rock-VR) with a melting agent (MA), $\text{CaCl}_2 \cdot 2\text{H}_2\text{O}$ at varying calcination temperature and MA/VR ratio ($w w^{-1}$). Measurement of extractable K in water (K_{water}), X-ray diffraction (XRD) and X-ray absorption near edge structure (XANES) were performed. The K_{water} increased up to 184-fold when the VR was calcined in presence of MA. Optimal condition for calcination of VR in terms of calcination temperature (850 °C) and ratio $w w^{-1}$ of MA/VR (1.7) promoted 95% K_{water} . Potassium K-edge XANES analysis revealed changes in the molecular environment of K due to the calcination of VR at increasing temperature. The fit to sylvite by K K-edge XANES analysis was supported by the detection of this mineral by XRD at temperature ranging from 700 to 900 °C. In addition, K K-edge XANES analysis indicated the gradual formation of a low crystalline potassium- silicate with increasing temperature,

fitted as low crystalline K_2SiO_3 (*lc*- K_2SiO_3). A joint analysis of data, including K_{water} and residue of Linear Combination Fitting analysis (LCF) suggested the formation of K mineral additional to sylvite and *lc*- K_2SiO_3 . The calcination process is effective in obtaining a highly soluble K specie from a low solubility raw material, and the end-products represent an alternative K fertilizer.

Key words: calcination, calcium chloride, glauconitic rock

1. Introduction

Potassium (K) is an essential element for plants and is required in large amounts in crop fertilization schemes. Underground deposits of soluble minerals such as sylvite (KCl), sylvinitite (KCl+NaCl), carnalite ($KMgCl_3 \cdot 6H_2O$) and langbeinite [$(K_2Mg_2(SO_4)_3)$] constitute the main sources of raw materials for the production of K fertilizers (Gowariker et al., 2009; Lima and Neves, 2014; Ott, 2012).

Global K fertilizer consumption is growing and estimates point for an annual increase in K fertilizer use around 3% until 2017 (IFA, 2013). Due to the scarcity of K ore deposits and the ever-growing demand for K fertilizers, alternative sources of K containing this element have become more relevant. Insoluble K silicate minerals, like micas and feldspars, are potential sources for the production of K fertilizers.

For the present study, we used a silicate potassium rock regionally called in Brazil as Verdete (VR). The reserve of this rock in Brazil is unknown, however in Cedro do Abaeté, Minas Gerais reserves of Verdete are estimated in 57.4 million tons (Alecrim, 1982). Glauconite and potassium feldspar are the main potassium minerals in this rock (Toledo Piza et al., 2011, Santos et al., 2015a). The concentration of K in glauconitic rocks, including VR with 7% w w⁻¹, can be considerable (Santos et al., 2015a), but its low solubility in water prevents the direct use of this rock as fertilizer (Toledo Piza et al., 2011; Santos et al., 2015a). Attempts to increase the water solubility of K in these materials have been made using chemical reagents and heating. Among these processes are, acid treatments (Yadav and Sharma, 1992; Santos, 2015b) and high calcination temperature (Mazumder, 1993; Santos et al., 2015b).

Regardless of the process, either based on heating or acid leaching, the resulting K species are a mix of materials varying from poorly to highly crystalline, thus requiring analytical techniques that are capable of detecting such species. X-rays diffraction (XRD) is widely used on the characterization of crystalline materials, whereby qualitative identification of minerals in heterogeneous materials can be achieved in a relatively easy manner. However, it lacks the ability to detect poorly crystalline phases. X-ray Absorption Near Edge Structure (XANES) spectroscopy is very sensitive to changes in molecular environment of absorber atoms, that can be used to characterize both amorphous and crystalline materials (Willmott, 2011).

Potassium K-edge XANES analysis has been used to investigate K speciation in different studies, including its transformation during pyrolysis and gasification of lignite (Huffman et al., 1992), in coal ash samples (Boni et al., 1988) and K coordination in trioctahedral micas (Cibin et al., 2005).

Our aim in this study was to investigate the effect of calcination of VR varying the temperature and ratio ($w w^{-1}$) of melting agent to VR (MA/VR). For that, water extractable K (K_{water}), XRD and K K-edge XANES analysis were performed.

2. Materials and methods

2.1. Preparation of samples

Verdete rock (VR) was collected in municipality of Cedro do Abaeté, state of Minas Gerais, Brazil. Samples of VR were taken from outcroppings at Geographic Coordinates UTM, $x= 426728.5970$; $y= 7881766.5310$. The VR were first ground in a rock mill and passed through a 150 μm sieve for chemical and mineralogical analysis and, calcination experiment.

2.2. Calcination experiment

To evaluate the reactivity of VR and changes in its mineralogy and in K species by calcination, was used as melting agent (MA) the calcium chloride ($\text{CaCl}_2 \cdot 2\text{H}_2\text{O}$). Calcium chloride was chosen due to its known performance to solubilize K-silicate rock (Manzumder, 1993; Nascimento, 2004), including the VR (Santos et al., 2015b). The calcination of VR was carried out by in a factorial combination (5×4) – five ratios ($w w^{-1}$)

MA/VR (0/1, 0.75/1, 1/1, 1.5/1 e 2.0/1) and four temperatures (500, 700, 900 and 1100 °C). The experimental units were arranged in a randomized complete design with three replications.

Samples ($\leq 150 \mu\text{m}$) of VR, were mixed with the respective quantities of MA. These mixtures (4.0 g) were placed in graphite crucibles and calcined in a muffle furnace, with a linear heating ramp for 45 min. When the final temperature was reached, the calcination time lasted for 60 min more. After calcination, the furnace was turned down and remained closed until room temperature ($\sim 25 \text{ }^\circ\text{C}$) was reached. Products of calcination were crushed using an agate mortar and passed through a $150 \mu\text{m}$ sieve.

2.3. Chemical analysis

Total K extraction from untreated VR and calcinated products was obtained by a tri-acid digestion (EPA 3052, 1996). In order to quantify the solubility of K in water (*K_{water}*), around 1.0 g of samples ($\leq 150 \mu\text{m}$) was transferred to a 125-ml Erlenmeyer flask and 50 mL of distilled water was added. The solution was boiled for 10 min in a heater plate. After cooling, the extract was filtered through slow quantitative filter paper ($\sim 28 \mu\text{m}$). The flasks were weighed before and after boiling in order to correct the volume. Potassium in the filtered extracts of both tri-acid digestion and *K_{water}* was quantified by flame emission spectrophotometry (Alcarde, 2009).

The *K_{water}* values were obtained by calculating the ratio ($w w^{-1}$) between their quantities extracted by water solution and their total concentration in the samples.

2.4. X-ray diffraction

Verdete rock samples were evaluated for their mineralogical compositions before and after calcination in the absence and presence of MA. X'Pert Pro MPD diffractometer (Panalytical) with Co-K α radiation ($\lambda = 1.789 \text{ nm}$) was used. The scan range was from 4 to 80° 2 θ , in 0.02° 2 θ steps at 1 step s $^{-1}$, 40 kV and 40 mA. Powder mounts were prepared by packing ground ($\leq 150 \mu\text{m}$) VR samples into aluminum holders. Only pure VR and 1/1 MA/VR ($w w^{-1}$) treatments were selected for XRD analysis. Minerals identification was performed using the *American Mineralogist Crystal Structure Database* (<http://rruff.geo.arizona.edu/AMS/amcsd.php>).

2.5. Potassium K-edge XANES

Potassium K-edge X-ray Absorption Near Edge Structure (XANES) measurements were performed at the Brazilian Synchrotron Light Laboratory (LNLS), in Campinas, Brazil. XANES data were collected at the Soft X-ray Spectroscopy (SXS) beamline using calcined samples of pure VR and 1/1 MA/VR ($w w^{-1}$), the same samples analyzed by XRD. A thin layer of the powdered ($\leq 75 \mu\text{m}$) material was uniformly spread on double-sided (K-free) carbon conductive tape and mounted on a stainless steel sample holder. The electron storage ring was operated at 1.37 GeV with a current between approximately 110 and 250 mA. The Si (111) double-crystal monochromator in the beamline was detuned by 20% to reject higher harmonics and calibrated to 2520 eV (E0), which represents the maximum in the first-derivative spectrum of a molybdenum foil (Mo L₃-edge). XANES data were collected in fluorescence mode with varying step sizes of 1.0 eV from 3579 – 3605 eV, 0.2 eV from 3605 – 3635 eV, 1.0 eV from 3635 – 3690 eV and 1.0 eV from 3690 – 3690 eV. Standards and reacted VR samples were diluted to 400 mmol kg⁻¹ of K in BN (Boron Nitrite) to avoid self-absorption.

Data analysis was performed using the Athena software in the computer package IFEFFIT (Ravel and Newville, 2005). Merged scans were normalized using a linear baseline function between -45 and -15 eV and a quadratic normalization function between 20 and 128 eV, both relative to E0 (~3608 eV). Linear Combination Fitting (LCF) analysis was performed using the Athena program using VR, non-crystalline potassium silicate (*lc*-K₂SiO₃), CAS N^o: 1312-76-1, and potassium chloride (KCl), CAS N^o: 747-40-7, as standards. Two approaches to fitting were used to determine the three best-fit standard spectra to the data: the standard-elimination approach described by Manceau et al. (2012), and fitting all possible combinations of up to three standards (Kelly et al., 2008).

3. Results

3.1. Changes in *Kwater*

Kwater is low for non-calcined VR, around 0.52% ($w w^{-1}$) of total K. Similar low *Kwater* is also observed for calcined VR when no MA is added ($\leq 1\%$ of total K) (Table 1). On the other hand, *Kwater* increased when VR was calcined in the presence of MA, with maximum *Kwater* at different temperatures and MA/VR ratio (Table 1). Modeling these

results, a quadratic response for K_{water} as a function of calcination temperature and MA/VR ratio, was yielded (Fig. 1). Based in this approach, highest K_{water} (95 % of total K) was reached at 1.7 MA/VR and temperature of 850 °C, increasing 183-fold the original K_{water} of untreated VR.

3.2. Changes in mineralogy and potassium speciation

X-ray diffraction revealed mineralogical changes in the VR due to increasing temperature (Fig. 2). Peaks of glauconite [$K_2(Mg,Fe)_2Al_6(Si_4O_{10})_3(OH)_{12}$] related to the 'c' dimension of the crystal (001) at 0.995 nm firstly became weaker with increasing temperature, then disappeared at 1100 °C and 700 °C, in the absence and presence of MA, respectively. At 1100 °C, in absence of MA, peaks of glauconite at 0.362, 0.299, 0.257, 0.216 and 0.197 nm were kept, as well as microcline ($KAlSi_3O_8$) at 0.649, 0.588, 0.497, 0.395, 0.378, 0.346, 0.322, 0.290, 0.251, 0.234 nm, and quartz (SiO_2) at 0.425, 0.334, 0.228, 0.223, 0.212, 0.202, 0.182 nm. On the other hand, in the presence of MA, glauconite was absent at 900 °C, whereas weak peaks of microcline were detected, eventually disappearing at 1100 °C (Fig. 2).

Peaks of sylvite (KCl) at 3.14 and 2.22 nm were detected at 700 °C, with greater intensity at 900 °C, disappearing at 1100 °C. Peaks of anorthite ($CaAl_2Si_2O_8$) at 0.403 and 0.207 nm were detected at 700 and 900 °C. The only mineral still found at 1100 °C in the presence of MA was quartz (Fig. 2).

The results showed the efficacy of $CaCl_2 \cdot 2H_2O$ as a melting agent, collapsing glauconite, microcline and quartz. In addition, we observed that sylvite and anorthite are new crystalline phases formed after calcination of VR mixed with MA, between 700 and 900 °C.

Changes VR colors were intense with temperature (Fig. 3). At the end of the calcination process, the original greenish VR became reddish when no MA was added, and yellowish in the presence of MA.

Following XRD and K_{water} , K K-edge XANES spectra revealed changes in K species following the increasing temperature (Fig. 4), indicating specific changes in chemical speciation of absorber atom (Willmott, 2011), i.e., changes in the local molecular coordination environments of K. The main changes in the spectra after heating in the presence of MA were related to the edge shoulder (~3610 eV), E_0 values, intensity and

energy of white line, post edge valley and weak peaks around of 3622, 3628, 3637 and 3638 eV, respectively. In the absence of MA, changes in K K-edge XANES spectra were lower and the spectra did not change much compared with the presence of MA. The disappearance of the 'd' signature indicates that the VR structure had broken, while the appearance of the 'c' weak peak suggests the formation of KCl, while the breaking down of the 'a' + 'b' signatures indicates the formation of K_2SiO_3 . The formation of KCl can also be viewed by XRD in the presence of MA at temperatures of 700 and 900 °C.

Linear Combination Fitting (LCF) analysis showed that heating VR at 500 °C is not enough to cause any significant change to VR, and 100% of K species remained as original VR, even in the presence of MA (Table 2). However, at 700 °C almost half of the K in the original VR had been converted to new mineral phases, fitted as low crystalline- K_2SiO_3 and KCl. As no K_2SiO_3 was detected by XRD but was found by XANES, we can assume that a non-crystalline form was produced. At 900 °C, K species distribution was nearly the same as for 700 °C. The amount of low crystalline- K_2SiO_3 by this fit, increased with increasing temperature. The 900 °C was the best temperature to produce KCl (Table 2).

Regression analysis considering results of LCF as a function of temperature, revealed that conversion of VR to new K species was linear with increasing temperature (Fig.5). Formation of KCl was best fitted by a quadratic model, indicating that 850 °C was the optimal temperature to form this K compound (Fig.5). This result is consistent with 850 °C being to optimum temperature for maximum *Kwater* (Fig.1).

A significant positive correlation was found between *Kwater* and concentration of KCl fitted by LCF analysis ($r= 0.92$), and there were not correlation with VR or *lc_K₂SiO₃* concentrations, when all temperatures were considered. However, when 1100 °C was not included in this analysis, negative correlation to VR ($r= -0.99$) and positive to *lc_K₂SiO₃* (0.99) became high and significant (Fig. 6). It means that the insoluble K species found in VR were being converted to soluble (KCl) and poorly soluble (*lc_K₂SiO₃*) K species with increasing temperature. In addition, after 900 °C the conversion to less soluble K species was intensified.

4. Discussion

Results indicate that the calcination of VR in absence of MA does not change significantly its solubility. Reaction with $\text{CaCl}_2 \cdot 2\text{H}_2\text{O}$ was essential to form water-soluble K species.

Calcination of VR in the absence of MA is not capable of promoting the formation of water-soluble K species. In fact, the increasing temperature from 500 to 1100 °C during the calcination process, without MA, lead to decreasing amounts of K_{water} . On the other hand, when MA was added K_{water} reached until up 95.7% of total K, confirming the effectiveness of CaCl_2 as a melting agent for silicate rocks (Mazumder, 1993; Nascimento, 2004; Santos et al., 2015b). The response surface indicates that the optimal condition to increase K_{water} from VR is to proceed with its calcination at 850 °C and a ratio (w w⁻¹) MA/VR of 1.7.

The decrease in K_{water} from 900 to 1100 °C (see Table 1 and Fig. 1) suggests the formation of less water-soluble K minerals, like K-rich spinel (produced at temperatures ~980 °C) and leucite (produced at temperatures ~1050 °C) (Rov, 1949; Tsvetkov and Valyashikhina, 1956). According to Mazumder (1993), crystalline KCl and CaO are formed with calcination of glauconitic rocks mixed with CaCl_2 . However, our XRD showed the formation only of KCl. Other phases, if formed, are low-crystalline.

Mashlan et al. (2012) showed that temperatures higher than 900 °C are necessary to collapse the glauconite structure. However, below this temperature the Fe^{+2} is oxidized to Fe^{+3} and the formation of hematite was observed, causing its colors to change. Similarly, we observed changes in VR colors during calcination. In the presence of MA, it became greenish to yellowish, and without MA it became from greenish to reddish (Fig. 3). However, we did not find any evidence of the presence of hematite by XRD analysis.

Like described above, XRD suggested that the glauconite was firstly collapsed in its (001) “*c*” dimension (Fig.2). Rov (1949) reported that there is a slight expansion in the ‘*c*’ dimension of muscovite when heated. Moreover, our K K-edge XANES analysis allowed us to track changes in the K molecular environment during calcination in absence of MA. According to Tedrow (1966) at 560 and 975 °C endothermic reactions in glauconite correspond the dihydroxylation of its structure. For trioctahedral micas, their thermal behavior is controlled by the octahedral and interlayer cations (Jackson 1975; Fanning et al.

1989). Based on the above, we think that the collapse of “*c*” dimension of glauconite with increasing the temperature associated the loss of structural hydroxyls decreases strain in the mica structure, and perhaps this changes the positions of siloxane oxygens or Si atom locations in relation to interlayer K^+ , then changing interatomic distances and consequently XANES spectrum.

Consistent with the increasing of K_{water} and mineralogical transformations, the presence of MA promoted intense changes in K species, as shown by “*a*, *b*, *c* and *d*” signatures of K K-XANES (see Fig. 3). In concordance with this perspective, the LCF analysis suggested the increasing of the soluble K species KCl, and *lc*- K_2SiO_3 (poorly soluble) with increasing of temperature. Supporting this interpretation, the XRD patterns confirmed the formation of secondary crystalline phases of KCl at 700 and 900 °C (see Fig. 2).

At 1100 °C, the amount of K species fitted as KCl decreased 1.7-fold when compared to 900 °C. In contrast, *lc*- K_2SiO_3 increased with increasing temperature up to 1100 °C (3-fold relatively to 900 °C). K_{water} decreased 2.8-fold from 900 to 1100 °C, when well-crystalline minerals present in VR, glauconite, quartz and microcline were disappearing. Like to demonstrated to *lc*- K_2SiO_3 , at 1100 °C the formation of less water-soluble K species was intensified. *lc*- K_2SiO_3 has low solubility in water ($\sim 0.1 \text{ g L}^{-1}$).

High residues found to LCF analysis, until to 0.04, at 700 °C for exemple, suggest that there are other K species were not used as standard to LCF analysis. Corroborating with this misfit, at 900 °C, 94% of K was water-soluble, but LCF analysis indicated that the participation of 48% of K species were from VR. However, VR has low water solubility. Only 0.52% ($w w^{-1}$) of total K from VR is soluble in water.

After all, our study shows the effectiveness of $CaCl_2$ as a MA in the calcination of VR, producing water-soluble potassium fertilizer from an insoluble, low-concentration and fairly abundant K source that currently does not have an industrial use. Future works in terms of economic viability, separation and concentration of K species should be explored to get more value products. Agronomic tests are needed to evaluate K uptake by plants and to compare with traditional sources of this nutrient.

5. Conclusions

The calcination process employed in a natural glauconite, K-rich metamorphic rock (verdete_VR) crushed efficient in obtaining a highly soluble K from an originally low solubility raw material, and the end-products might represent an alternative source of K for fertilizer production. Calcination of VR in the absence of MA, was not effective to increasing the solubilized K in water. With MA/VR ratio ($w w^{-1}$) was equal to 1.7, at 850 °C, 95% of total K became extractable. Potassium K-XANES analysis revealed changes in K species due to the calcination of VR, with formation of secondary K species, fitted as KCl and *low crystalline*-K₂SiO₃. Moreover, this analysis indicates that there are unknown K species formed in presence of MA, which we did not use as standards. Further studies on the economic viability, separation and concentration of K species should be explored to provide a better assessment of end-products. Agronomic tests are also needed to evaluate K uptake by plants and to compare with traditional sources of this nutrient.

Acknowledgment

The authors gratefully acknowledge funding received from FAPEMIG (APQ-04092-10), CAPES (A105/2013), and the Brazilian Synchrotron Light Laboratory (LNLS), in Campinas, Brazil.

References

- Alecrim, J. D. (1982): Recursos minerais do Estado de Minas Gerais. METAMIG, Belo Horizonte, Brasil p. 299.
- Boni, A. A., Helble, J. J., Srinivasachar, S., Sarofim, A. F., Beer, J. M., Peterson, T. W., Wendt, O. L., Huffman, G. P., Huggins, F. E. (1989): Transformations of inorganic coal constituents in combustion systems. Proceeding AR and TD Contractors Reviwing Meeting. 2, 497-536.
- Cibin, G., Mottana, A., Marcelli, A., Brigatti, M. F. (2005): Potassium coordination in trioctahedral micas investigated by K-edge XANES spectroscopy. Miner Petrol. 85, 67-87.

- EPA, L. (1996): Microwave assisted acid digestion of siliceous and organically based matrices. Method.
- Fanning, D. S., Keramidas, V. Z., El-Desoky, M. A. (1989): Micas. In Dixon, J B and Weed, S B: Minerals in soil environments. Soil Science Society of America: Madison, Wisconsin, USA, 551-634.
- Gowariker, V., Krishnamurthy, V., Gowariker, S., Dhanorkar, M., Paranjape, K. (2009): The fertilizer encyclopedia. John Wiley & Sons. p. 880.
- Huffman, G., Huggins, F., Shah, N. (1992): XAFS spectroscopy studies of critical elements in coal and coal derivatives. In Meuzelaar, HCL. Advances in Coal Spectroscopy. Plenum Press, New York. 29-47.
- IFA (2013): 81st IFA Annual Conference Chicago (USA)_Fertilizer Outlook 2013-2017. International Fertilizer Industry Association: Chicago, USA. Available at: http://www.fertilizer.org/imis20/images/Library_Downloads/2013_chicago_ifa_summary.pdf. Accessed: 19 May, 2014.
- Jackson, M. L., Barak, P. (2005): Soil chemical analysis- Advanced course. UW-Madison Libraries Parallel Press, University of Wisconsin, Madison, USA.
- Kelly, S. D., Hesterberg, D., Ravel, B. (2008): Analysis of soils and minerals using X-ray absorption spectroscopy. Methods of soil analysis. Part. 5, 387-463.
- Lima, T. M., Neves, C. A. R. (2014): Sumário Mineral 2012. In Departamento Nacional de Produção Mineral, DNPM. DNPM: Brasilia, 141.
- Manceau, A., Nagy, K. L. (2012): Quantitative analysis of sulfur functional groups in natural organic matter by XANES spectroscopy. Geochim Cosmochim Ac. 99, 206-223.
- Mashlan, M., Martinec, P., Kašlík, J., Kovářová, E., Scucka, J. (2012): Mössbauer study of transformation of Fe cations during thermal treatment of glauconite in air. Spectroscopy. 1, 5-7.
- Mazumder, A., Sharma, T., Rao, T. (1993): Extraction of potassium from glauconitic sandstone by the roast-leach method. Int J Miner Process. 38, 111-123.
- Nascimento, M. (2004): Desenvolvimento de método para extração de potássio a partir de feldspato potássico. Tese de Doutorado, Universidade Federal do Rio de Janeiro, Brasil., Rio de Janeiro, Brasil.

- Ott, H. (2012): Fertilizer markets and their interplay with commodity and food prices. JRC Scientific and Policy Reports. 1-34.
- Ravel, B., Newville, M. (2005): ATHENA, ARTEMIS, HEPHAESTUS: data analysis for X-ray absorption spectroscopy using IFEFFIT. J Synchrotron Radiat. 12, 537-541.
- Rov, R. (1949): Decomposition and resynthesis of the micas. J Am Ceram. 32, 202-209.
- Santos, W., Mattiello, E. M., Costa, L. M., Abrahão, W. A. P (2015 a): Characterization of verdete rock as a potential source of potassium. Revista Ceres. 62, 392-400.
- Santos, W. O., Mattiello, E. M., Costa, L. M., Abrahão, W. A. P., Novais, R. F., Cantarutti, R. B. (2015 b): Thermal and chemical solubilization of verdete for use as potassium fertilizer. Int J Miner Process. 140, 72-78.
- Tedrow, J. (1966): Properties of sand and silt fractions in New Jersey soils. Soil Science. 101, 24-30.
- Toledo Piza, P. A., Bertolino, L. C., Silva, A. A. S., Sampaio, J. A., Luz, A. B. (2011): Verdete da região de Cedro de Abaeté (MG) como fonte alternativa para potássio. Geociências. 30, 345-356.
- Tsvetkov, A. I., Valyashikhina, E. P. (1956): Bull Acad Sc. USSR, Ser. Geol. 5, 74-83.
- Willmott, P. (2011): An introduction to synchrotron radiation: techniques and applications. John Wiley & Sons.
- Yadav, V., Sharma, T. (1992): Leaching of glauconitic sand stone in acid lixivants. Minerals engineering. 5, 715-720.

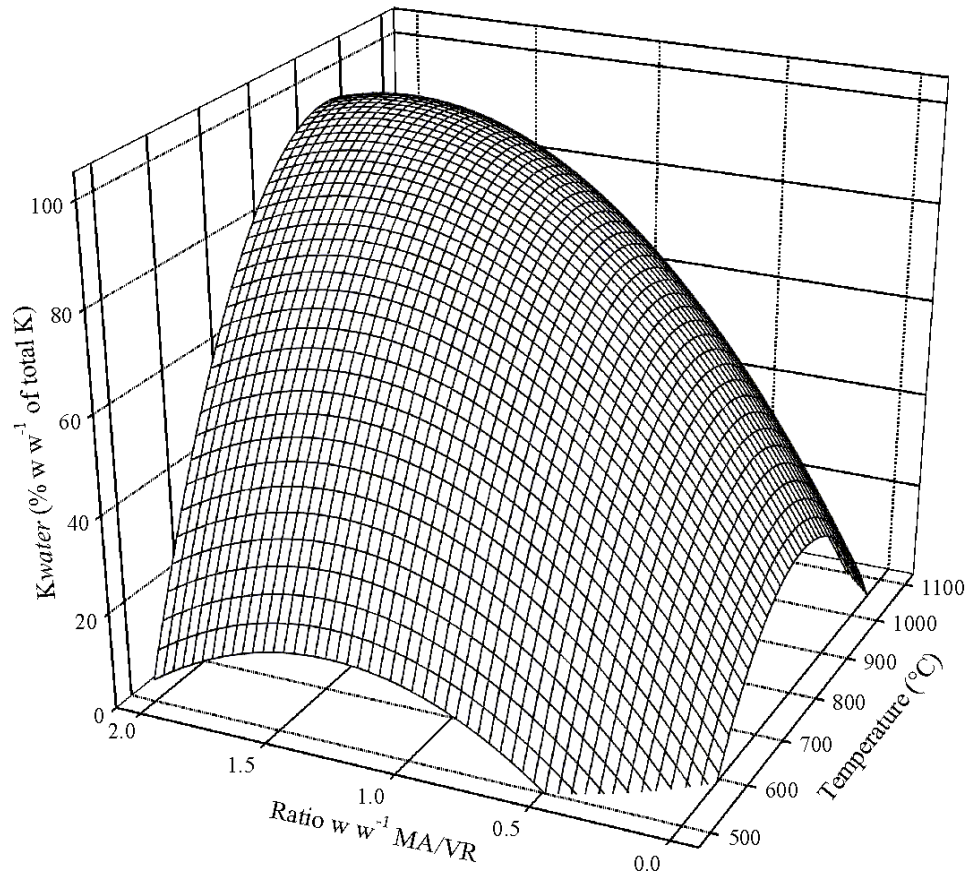
Table 1. Extractable K in water (K_{water}) for calcined Verdete Rock (VR) mixed with a melting agent (MA), $\text{CaCl}_2 \cdot 2\text{H}_2\text{O}$, at different temperatures and ratios (w w^{-1}) MA/VR

Temperature	-----Ratio w w^{-1} , MA/VR-----				
	0	0.75	1	1.5	2
	----- (% , w w^{-1} , of total K)-----				
Non-calcined VR	0.5				
500 °C	0.8	1.9	2.2	2.8	2.6
700 °C	1.0	69.4	78.7	86.3	95.7
900 °C	0.5	82.9	93.7	95.1	88.8
1100 °C	0.3	1.3	33.6	48.3	39.3

Table 2. Combinations of natural Verdete Rock (VR), potassium chloride (KCl) and low crystalline potassium silicate (*lc*-K₂SiO₃) standards yielding the best fits (Linear Combination Fitting) to Potassium K-edge XANES spectra of VR subjected the calcination in the presence of a melting agent (MA), CaCl₂.2H₂O at 1/1 MA/VR

Sample	Standards			R-factor(†)
	VR	KCl	<i>lc</i> -K ₂ SiO ₃	
α	----- (%) -----			-
500 °C+MA*	100	0	0	-
700 °C+MA	55±3	32±5	13±5	0.040
900 °C+MA	48±3	38±5	14±5	0.030
1100 °C+MA	22±1	23±2	55±2	0.004

† R-factor = $\frac{\sum(\text{data}-\text{fit})^2}{\sum(\text{data})^2}$, is a measure of the residual in the fit.*The used samples correspond the treatments in ratio (w w⁻¹) MA/VR equal 1/1.



$$\hat{y} = -412 + 43.16^{**}p + 1.12^{**}t - 21.09^{**}p^2 - 0.000699^{**}t^2 + 0.034^*p.t \quad (R^2 = 0.81)$$

Fig. 1. Response surface fitted by multiple regression analysis that represent *Kwater* as a function of calcination temperature and ratio ($w w^{-1}$) between a melting agent (MA), $\text{CaCl}_2 \cdot 2\text{H}_2\text{O}$, and the Verdete Rock (VR), (MA/VR). Superscript astericks (“^{*}”, “^{**}”) indicate statistical significance at the 5 and 1% probability, respectively according to a *t* test.

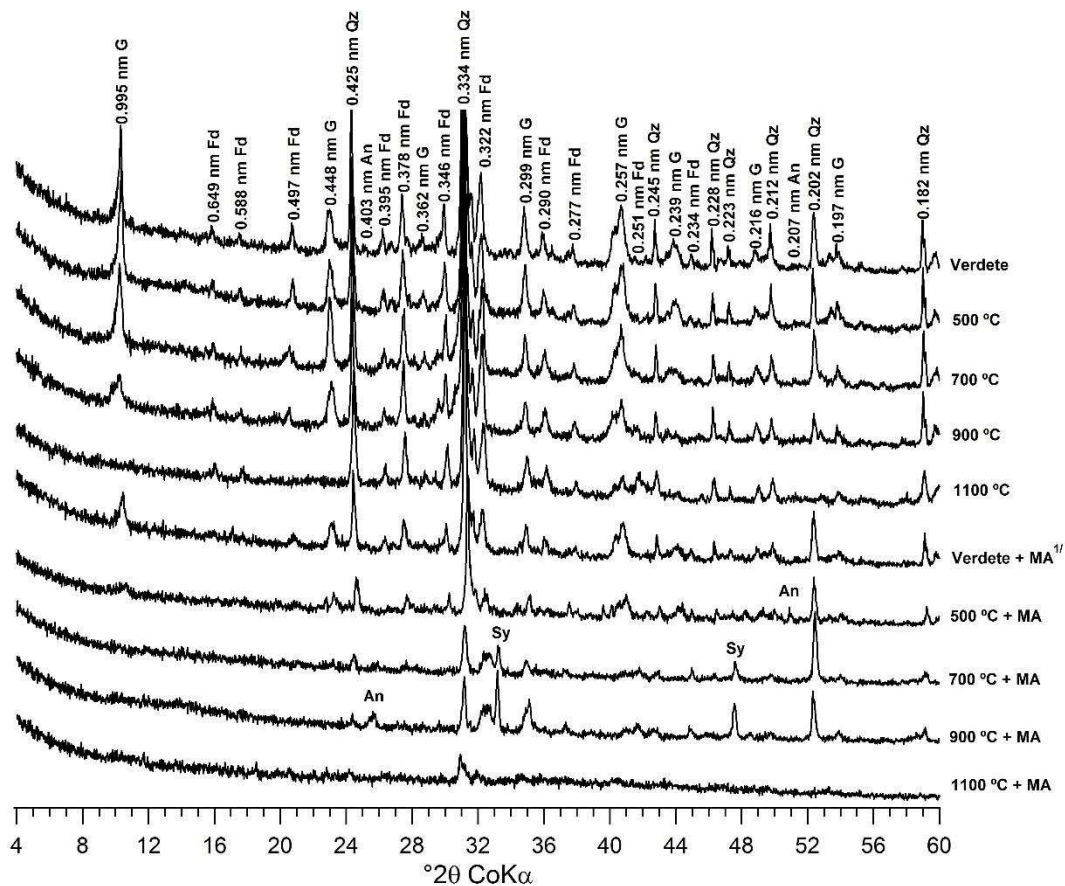


Fig. 2. X-ray diffraction patterns of VR subjected to calcination in the presence and absence of a melting agent (MA), $\text{CaCl}_2 \cdot 2\text{H}_2\text{O}$, and the Verdete Rock (VR) in various calcination temperature. G: glauconite [$\text{K}_2(\text{Mg,Fe})_2\text{Al}_6(\text{Si}_4\text{O}_{10})_3(\text{OH})_{12}$]; Qz: quartz (SiO_2); Fd: feldspar potassic, microcline [$(\text{KAlSi}_3\text{O}_8)$]; Sy: sylvite (KCl) and An: anorthite ($\text{CaAl}_2\text{Si}_2\text{O}_8$). Data were collected using $\text{Co K}\alpha_1$ radiation (1.789 Å). *The used samples correspond the ratio (w w⁻¹) MA/VR equal 1/1.

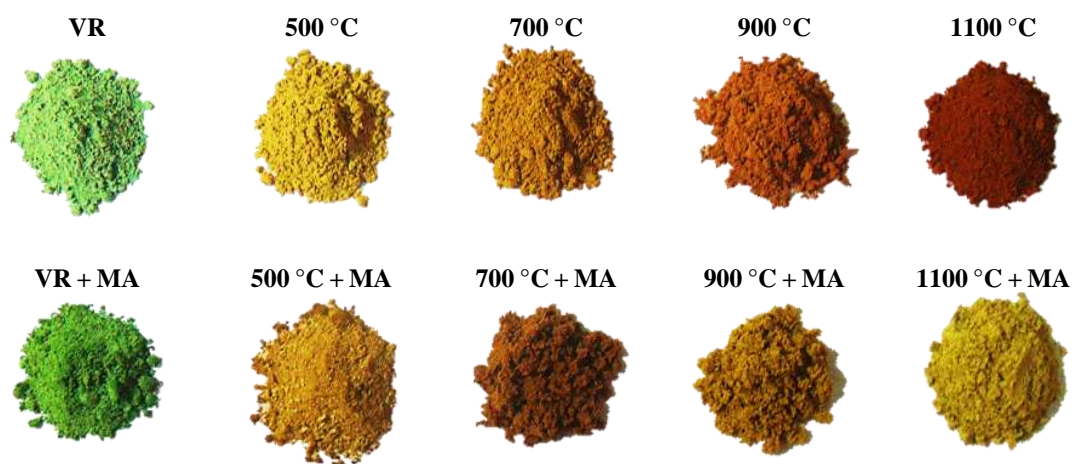


Fig. 3. Changes in color of verdete rock (VR) in absence and presence of a melting agent, $\text{CaCl}_2 \cdot 2\text{H}_2\text{O}$ (+MA), 1/1 ratio MA/VR (w w⁻¹), varying calcination temperature.

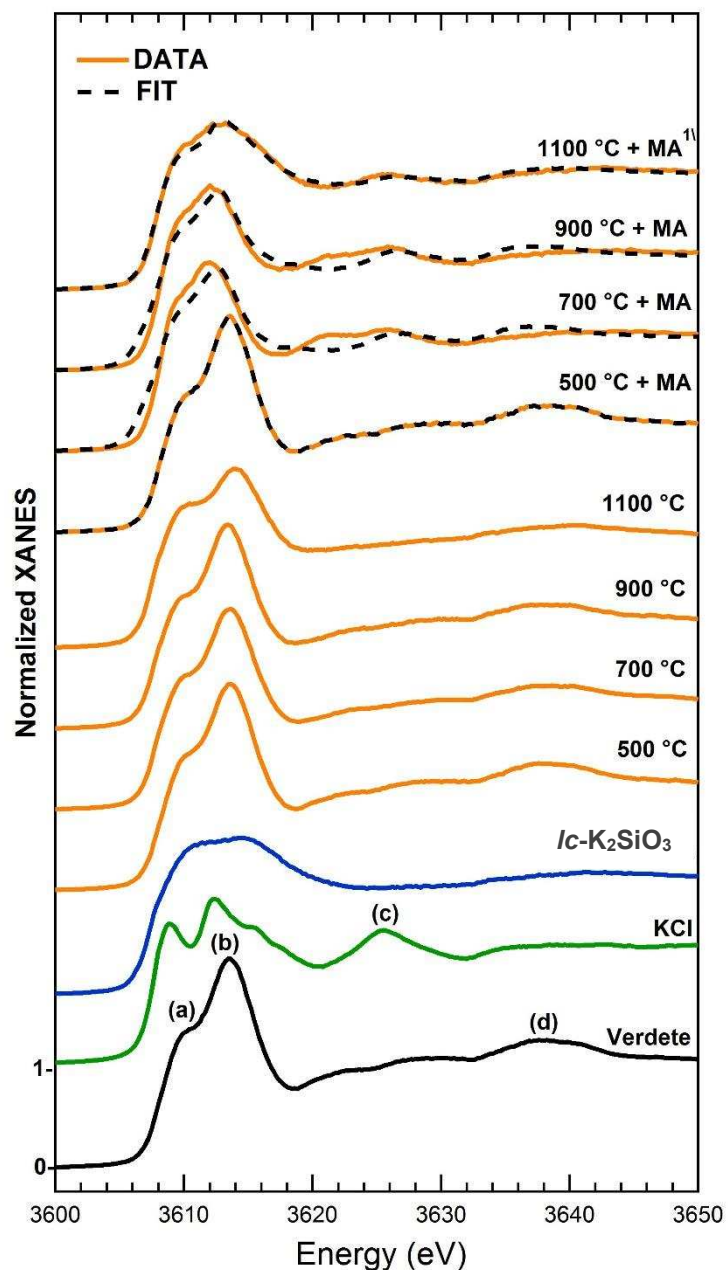


Fig. 4. Stacked, normalized K K-edge XANES spectra for VR calcined in the presence of a melting agent (MA), $\text{CaCl}_2 \cdot 2\text{H}_2\text{O}$. The natural Verdete Rock (VR), potassium chloride (KCl) and low crystalline potassium silicate ($lc\text{-K}_2\text{SiO}_3$) represent the potassium standards used to perform the Linear Combination Fitting analysis. The selected treatments were corresponding the ratio MA/VR (w w^{-1}) equal 1/1. Potassium K-XANES spectra, including (a), (b), (c) and (d) signatures represent the average of environment of molecular coordination of K.

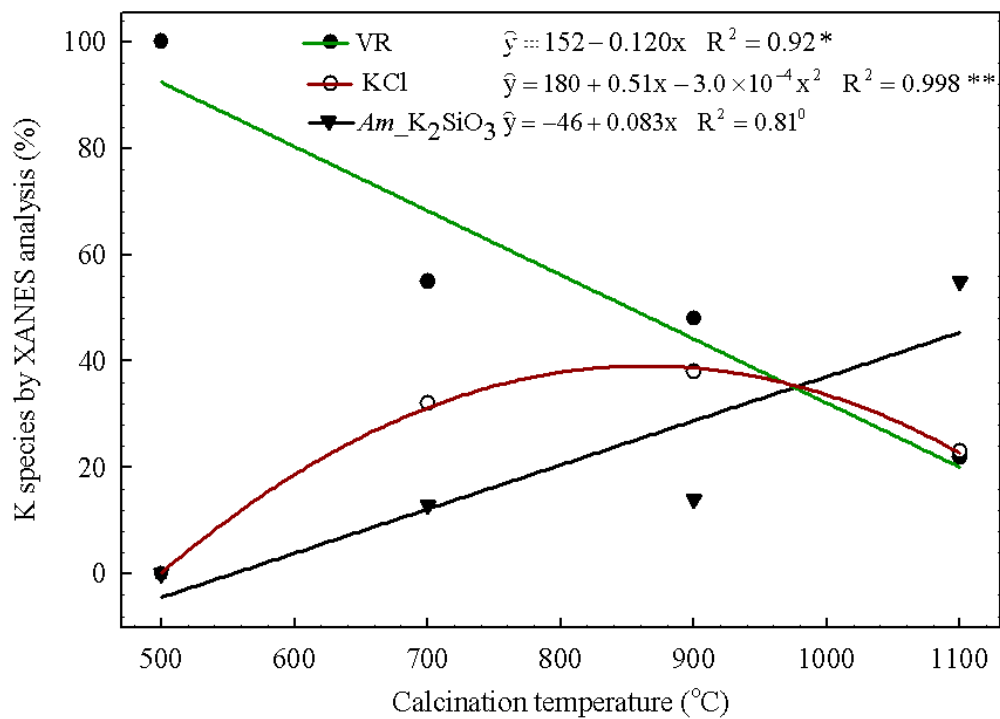


Fig. 5. Relationship between the increasing of calcination temperature and the abundance of K species fitted by K K-XANES analysis. VR, Verdete Rock. Superscript zero (°) and asterisks (*, **) indicate statistical significance at the 10, 5 and 1% probability, respectively according to the *t* test.

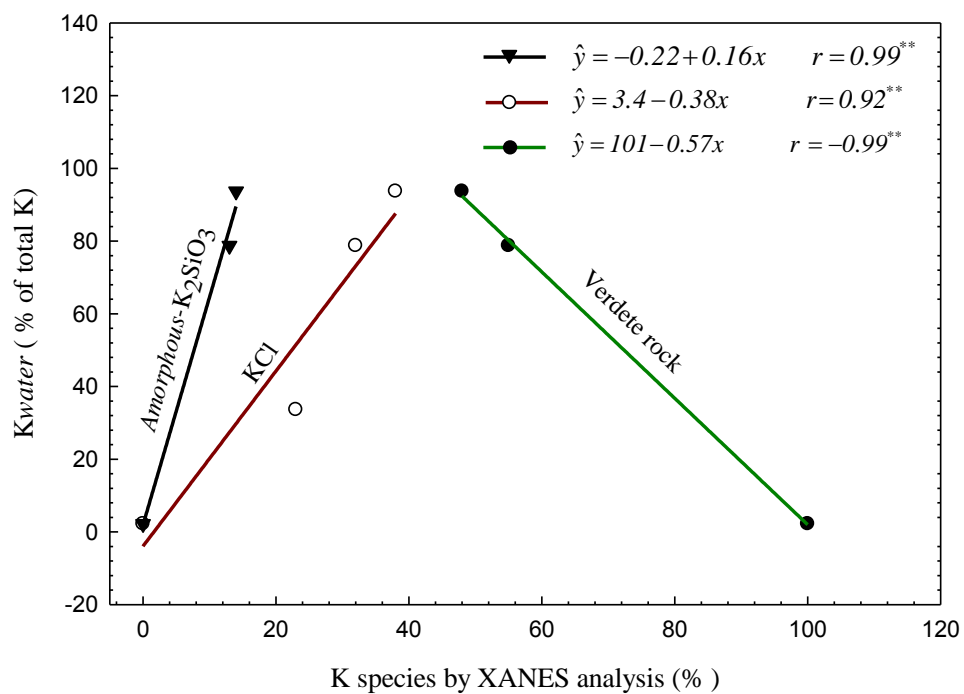


Fig. 6. Pearson correlation analysis considering the *Kwater* and abundance (%) of K species fitted by XANES analysis. Asterisks (*, **) indicate statistical significance at the 5 and 1% probability, respectively according to a *t* test. Significant correlations were found to low crystalline potassium silicate (*lc-K₂SiO₃*) and Verdete rock for temperatures of 500, 700 and 900 °C. For KCl standard, the significance occurred including all of calcination temperatures.

ARTIGO 2

Increasing soluble phosphate species by treatment of phosphate rocks with acidic mine waste

Wedisson Oliveira Santos*¹, Dean Hesterberg², Edson Marcio Mattiello¹, Leonardus Vergütz¹, Matheus Sampaio Carneiro Barreto¹, Luiz Francisco da Silva Souza-Filho¹, Ivo Ribeiro da Silva¹

1 Department of Soil Science, Universidade Federal de Viçosa (UFV), Av P. H. Rolfs, Viçosa, Minas Gerais, Brazil, CEP 36570-000

2 Department of Soil Science, PO Box 7619, North Carolina State University, Raleigh, North Carolina, United States, 275695-7619

Abstract

The development of efficient, environmentally friendly fertilizers will help in meeting the increasing demand for food and nutrients by a growing global population. Our objective was to evaluate whether an acidic mine waste (AMW) could be used beneficially by reacting it with sparingly soluble phosphate rocks (PRs) to produce more soluble P fertilizer materials. Three PRs from Brazil or Peru were reacted with different concentrations of AMW. Changes in mineralogy and P species were determined using a combination of X-ray diffraction (XRD) and phosphorus K-edge XANES spectroscopy, in addition to extractable P concentrations. Increasing AMW concentration typically increased P extractable. XRD data showed the disappearance of apatite when PRs were reacted with AMW at $\geq 50\%$. Gypsum or anhydrite were formed at AMW concentrations as low as 12.5%. Linear combination fitting analysis (LCF) also showed apatite disappearance with increasing AMW concentrations, and the progressive formation of up to 79% of Fe (III)-bound phosphate, fitted as amorphous FePO_4 . Moreover, LCF indicated that the addition of AMW produced up to 30% of a more soluble Ca-phosphates phase. Our results showed that an acid mining waste that is very costly to dispose is an alternative to the industry standard of pure acids used to produce phosphate fertilizers from PRs.

Key words Acidification. Natural Phosphate. Phosphorus K-XANES. Residue. Reuse.

Introduction

A reliable supply of phosphate fertilizers is essential for agriculture to continually meet increasing worldwide food demands. Commercial phosphate fertilizers are usually manufactured by the wet reaction of rock phosphates (PRs) with pure acids (*Chien et al.* 2011). The quality of mined PRs used as a raw material for phosphorus fertilizer (P-fertilizer) production is highly variable because the mineralogy, chemical composition, and reactivity of these materials depend on the geological conditions of formation (*Chien and Menon* 1995; *Chien et al.* 2003). A projected scarcity of high-grade P sources and regional aspects of resource availability have stimulated scientific and economic interest in more efficient and cost-effective P-fertilizer production and P-recovery technologies (*Cordell et al.* 2011).

New processes for converting PRs into high-grade phosphate fertilizers are needed to help maintain a steady, cost-effective supply of this critical plant macronutrient.

According to *Nriagu and Moore (1984)*, there are about 350 known phosphate minerals. Within this group, apatites $[\text{Ca}_{10}(\text{PO}_4)_6\text{X}_2]$ are the most important form of phosphorus (P) in PRs used in fertilizer production. The manufacture of phosphate fertilizers involves acidification to induce proton attack on the apatite structure. The reactivity of the PRs depends on the component “X” in the structural formula of the apatite, which can be F^- , Cl^- , or OH^- ; and the degree of isomorphic substitution of CO_3^{2-} for PO_4^{3-} (*Chien et al. 2011; Lehr 1980, 1984; Young 1974*). The “X” ions in apatite crystals are more susceptible to proton attack because of their location in calcium (Ca) channels parallel to the c-axis, and acid dissolution begins with the detachment of these ions from apatite surfaces (*Young 1974; Dorozhkin 1997, 1999, 2012*). Many factors, however, influence the kinetics of apatite dissolution; including rock composition, particle size, crystallinity, crystal defects, composition and strength of the reacting acid, temperature, and hydrodynamics (*Chien et al. 2011; Dorozhkin 2012*).

Common acids used to solubilize apatite to produce soluble phosphate fertilizers include sulfuric acid (H_2SO_4), phosphoric acid (H_3PO_4), and nitric acid (HNO_3). Acidification ideally forms monocalcium phosphate $[\text{Ca}(\text{H}_2\text{PO}_4)_2]$, which is highly soluble in water (20 g/L) (*Chien et al. 2011; Lehr 1984*). However, the complexity of PR matrices may result in intermediate compounds with unknown characteristics being produced during acidification (*Dorozhkin 2012*) and the solubility of these intermediate phosphate compounds affects the quality of the phosphate fertilizers produced (*Chien et al. 2011; Chien and Menon 1995; Lehr 1984; Dorozhkin 2012*).

As an alternative to using pure acids to produce high-grade P-fertilizers, this research focuses on reacting a waste acid from a mining operations with PRs. Such beneficial use of an industrial waste stream could decrease the costs of both fertilizer production and waste disposal, while diminishing negative environmental impacts of waste acid disposal. The management of industrial wastes to comply with legal standards is expensive, and efforts are on the rise to develop technologies that minimize waste generation and increase recycling and reuse (*Capón-García et al. 2014; Puig et al. 2013; Mattiello et al. 2015*). As a feedstock for industrial production of P-fertilizers, waste acids contain impurities such as Fe, Mn, K,

Al, SO₄, and trace elements (Ni, F, Pb, and Cd). Reaction of these components with PRs could produce unknown intermediate compounds that affect the quality of fertilizers produced. Consequently, research is needed to assess the solubility and speciation of fertilizers produced by reacting PRs with waste acids from mining operations.

Speciation of P in complex matrices can be achieved using synchrotron X-ray absorption near edge structure (XANES) spectroscopy (*Beauchemin et al.* 2003; *Hesterberg et al.* 1999; *Toor et al.* 2006; *Lombi et al.* 2006). Phosphorus K-edge XANES analysis can provide information about composition, transformation and solubility of P species based on unique spectral signatures obtained when H_xPO₄^{x-3} is bonded with different cations like Al³⁺, Fe³⁺ and Ca²⁺ in minerals, amorphous solids, and adsorbed species (*Beauchemin et al.* 2003; *Diaz et al.* 2008; *Hesterberg et al.* 1999; *Ingall et al.* 2010; *Kar et al.* 2012; *Kizewski et al.* 2011; *Lombi et al.* 2006; *Prietzl et al.* 2013). Although P K-edge XANES has been applied to soils and animal wastes (*Toor et al.* 2006; *Sato et al.* 2005; *Prietzl et al.* 2013; *Hesterberg et al.* 1999; *Beauchemin et al.* 2003) its use in developing fertilizer technologies has been limited to only a few studies (*Lombi et al.* 2006; *Khatiwada et al.* 2012).

Our goal is to develop an alternative route of P-fertilizer production using an acidic mining waste (AMW). The specific objective of this research was to analyze transformation products and the extractability of P in materials produced by reacting AMW with PRs. Measurements of chemical composition, P extractability by reagents used to evaluate fertilizer quality, bulk mineralogy, and P speciation by XANES analysis were made on PRs that were reacted with varying concentrations of AMW diluted in water.

Materials and methods

Phosphate Rocks (PRs)

Two Brazilian PRs (Araxá and Patos) and one Peruvian PR (Bayóvar) were used in this study. Araxá and Patos PRs are deposits located in the state of Minas Gerais in Brazil, and the Bayóvar PR is from the Sechura Desert in Peru. Araxá PR is from an igneous deposit, and Patos PR is from a sedimentary deposit with a high degree of metamorphism. The elements Fe, Al, Mn, Zn, Ni, Pb, Cu, Cr, and Cd were determined in PRs samples digested for total elemental analysis (*Alcarde* 2009) using inductively coupled plasma optical emission spectrometry (ICP-OES) (PerkinElmer, Optima TM 4300DV). The P in Araxá and

Patos PRs had been concentrated before we received them from Bunge Fertilizantes S.A and Ultrafertil S.A companies, respectively. Araxá and Patos PRs are normally not suitable for direct use as phosphate fertilizer due to the low P solubility, but are used as raw materials to produce high-grade fertilizers by thermal or wet acidification processes (*Beisiegel and Souza 1986; Lapido-Loureiro and Melamed 2006; Oba 2004; Prochnow et al. 2004*). Bayóvar PR is from a marine sedimentary deposit, and is used as a raw material in fertilizer production without pre-concentration. We received Bayóvar PR from Heringer Fertilizantes S.A. This PR has a high degree of isomorphic substitution of carbonate for phosphate and is more soluble than the Brazilian PRs. It is an adequate material for direct application to soils as a P fertilizer, but it is less effective than high-grade phosphate fertilizers for annual crops (*Faria and Guardieiro 2011*).

Acidic mining waste (AMW)

The AMW used in our experiments to solubilize PR is produced by the company London Scandinavian Metal Brasil S.A., located in the city of São João Del Rei in Minas Gerais State, Brazil. The AMW is a residue generated from the extraction of tantalum (Ta) and niobium (Nb) oxides from pegmatite ores using a mixture of H₂SO₄, HF, and HCl. This process generates approximately 17,250 m³ of AMW effluent and 12,700 tonnes of mud annually, which must be neutralized before disposal into special landfills. These wastes currently constitute an important part of the company's environmental liability. As with PRs digests, Fe, Mn, Al, K, Ca, Mg, Ni, Cu, Pb, Zn, Cr, and Cd were determined in AMW samples using ICP-OES. The anions Cl⁻, F⁻, SO₄²⁻, NO₃⁻, PO₄³⁻, and Br⁻ from AMW, were quantified by ion chromatography (DX500; Dionex, Sunnyvale-CA), with chemically suppressed detection of electric conductivity by using a mobile phase gradient; consisting of ultra-pure water, methanol, and 0.1 mol L⁻¹NaOH, as proposed by *Silva et al. (2001)*.

Experimentation

A 3 x 5 factorial design was used for P acidification experiments, including the three PRs (Araxá, Patos and Bayóvar) and four AMW concentrations (12.5, 25, 50, and 75% v v⁻¹ in H₂O) along with non-treated PR as a control (designated 0% AMW treatment). Non-treated PRs means that was used only distilled water on the control treatment. Treatments

were blocked in time into three randomized complete blocks. All PRs were first ground and passed through a 150 μm sieve (100 mesh). Five grams of each PR sample were reacted with 20 mL of each concentration of AMW in 50 mL centrifuge tubes by shaking at 25 $^{\circ}\text{C}$ for 60 min at 150 rpm on a horizontal reciprocating shaker. After shaking, uncapped tubes were heated to 80 ± 5 $^{\circ}\text{C}$ for 4 h in a water bath to decrease the F concentration by volatilization. The materials were transferred to glass beakers and dried in an airflow oven at 105 $^{\circ}\text{C}$ for 72 h. The cooled solids were again ground to pass through a 150 μm sieve to produce our alternative fertilizer materials.

Chemical characterization

Total P concentrations (P_{total}), and fractions of water soluble P (P_{water}), neutral ammonium citrate soluble P (P_{NAC}), and citric acid soluble P (P_{AC}) were measured in non-treated (0% AMW) and treated PRs samples (*Alcarde 2009*) used for phosphate fertilizer characterization. Phosphorus concentrations in aqueous solutions were determined spectrophotometrically using the yellow phosphovanadomolybdate-complex method (*Wright and Stuczynski 1996*).

X-ray diffraction (XRD) analysis

AMW-treated and non-treated PRs samples were evaluated for mineralogical composition using an X'Pert Pro MPD diffractometer (Panalytical) and Co-K α radiation ($\lambda = 1.7889$ \AA) produced at 40 kV and 30 mA. Powder mounts were prepared by packing ground samples (≤ 150 μm) into aluminum holders. The scan range was from 4 to 80 $^{\circ}$ 2 θ , in 0.02 $^{\circ}$ 2 θ steps at a rate of 1 step s^{-1} . Minerals identification was performed using the *American Mineralogist Crystal Structure Database* (<http://rruff.geo.arizona.edu/AMS/amcsd.php>).

Phosphorus K-edge XANES analysis

Treated and non-treated samples of PR were ground to ≤ 75 μm (200-mesh) for P K-edge XANES analysis. A thin layer of the powdered material was uniformly spread on double-sided (P-free) carbon conductive tape and mounted on a stainless steel sample holder. XANES data were collected at the Soft X-ray Spectroscopy (SXS) beamline at the Brazilian Synchrotron Light Laboratory (LNLS) in Campinas, Brazil. The electron storage ring was

operated at 1.37 GeV with a current between 100 and 300 mA. The Si(111) double-crystal monochromator on the beamline was detuned by 20% to reject higher harmonics and calibrated to an energy (E_0) of 2,151.2 eV at the maximum in the first-derivative spectrum of a monocalcium phosphate standard. XANES data were collected in fluorescence mode between 2,110 and 2,445 eV, with varying step sizes of 1.0 eV from 2,110 – 2,143 eV, 0.2 eV from 2,143 – 2,185 eV, 1.0 eV from 2,185 – 2,255 eV, and 5.0 eV from 2,255 – 2,445 eV. Standards and reacted PR samples were diluted to 50 mmol/kg of P in BN (boron nitride) to avoid self absorption (*Kelly et al.* 2008).

Data analysis was performed using the IFEFFIT package in the Athena computer software (*Ravel and Newville* 2005). Merged scans were normalized using a linear baseline function between -20 and -9 eV relative E_0 (~2151 eV) and a quadratic normalization function between 32 and 59 eV above E_0 , including use of the “flatten” feature in Athena. Linear-combination fitting (LCF) analysis was performed using the Athena software. Two approaches to LCF analysis were used. In the first approach, spectra for samples from the 12.5 and 25% AMW treatments were fit with those of the 0 and 75% AMW treatments to determine whether there was a progression of P species transformation with increasing AMW treatment. In the second approach, samples were fit using 19 purchased or synthesized standards of Fe-, Al-, and Ca-bonded phosphates, most of which were previously published (*Beauchemin et al.* 2003; *Hesterberg et al.* 1999; *Khare et al.* 2005). The original (non-treated, 0% AMW treatments were used as the hydroxyapatite standard, and an amorphous Ca-phosphate (“ACP”) standard reported by *Eveborn et al.* (2009) was also included. The LCF analysis was conducted over a spectral range from -7 to +35 eV relative to E_0 , the first-derivative maximum of each sample or standard at ~2151 eV. For fitting with the full set of standards, we used both the standard-elimination method described by *Manceau and Nagy* (2012) and fitting with all possible combinations of up to three standards (*Kelly et al.* 2008) to select the fits that were most consistent between methods. The energy scales of the standards were allowed to shift by a maximum of +/- one energy step (± 0.2 eV).

Results

Chemical composition of PRs and AMW

All three PR (0 % AMW) used here contained 29-30% (w w⁻¹) P₂O₅, but varied in concentrations of Fe, Al, Mn, and cationic trace elements (Table 1). The Araxá PR sample contained 1.2- and 4.8-fold more Fe than the Bayóvar and Patos PRs, respectively, but less Al (Table 1).

The AMW reacted with the PRs used here was very acidic, and required 5.75 moles of NaOH to neutralization from pH ~ 0 to 7 (Table 2). The AMW also contained elevated concentrations of Fe, Mn, Cr, Ni, Pb, and Cd (Table 2). The acidity and trace-element concentrations make the AMW unsuitable for direct discharge into water bodies according to current waste-discharge standards adopted by the Brazilian legislation (*BRASIL* 2011).

AMW-Induced Changes in Extractable Phosphorus

The proportions of total P in the original (non-treated) and AMW-treated PRs that were dissolved in water, neutral ammonium citrate, or citric acid (P_{water}, P_{NAC}, or P_{CA}) are shown in Table 3 and plotted in Fig. 1. These operational extractants provided a metric for changes in P solubility and potential plant availability following treatment with AMW. For fully acidified P fertilizer, values of sequential extraction of P_{water} and P_{NAC} has been related to plant-available P (*Chien et al.* 2011). According to these authors, the water-insoluble but citrate-soluble compounds present in these P fertilizers do have some agronomic value when compared to compounds that are 100% water soluble such as MCP. In terms of P available to plants, agronomic performance is different for various fertilizers with low contents of P_{water}.

For most samples, extractable P increased in the order P_{water} < P_{NAC} < P_{CA}, especially for AMW treatments of <50% (v v⁻¹). Both P_{water} and P_{NAC} for the non-reacted PRs were considered to be low (≤0.7 and ≤ 2.4% w w⁻¹), but increased by up to 526-fold (P_{water}) and up to 42-fold (P_{NAC}) when treated with AMW, respectively. Citric-acid extractable P increased only by up to 3-fold, but already constituted 15 to 36% (w w⁻¹) of total P in the non-treated PRs (Table 3). In general, extractable P increased linearly with increasing concentration of AMW, except for the Patos PR where the best fit was quadratic (Fig. 1). Based on the linear models, treatment with our maximum evaluated concentration of a 75%

(v v⁻¹) solution of AMW yielded the greatest proportion of all three extractable P concentrations for Araxá and Bayóvar PRs. Based on derivatives of the quadratic models for Patos PR, AMW concentrations of 45, 62, and 47% (mean = 51 ± 9%) produced the maximum P_{water}, P_{NAC}, and P_{CA} for this PR (Table 3, Fig. 1). These results indicate that PRs acidification by AMW can increase the fertilizer value of PRs by increasing plant available P. Although higher solubility of phosphate fertilizers can improve agronomic efficiency, factors such as soil properties, management practices, and cultivated species also affect plant availability (Chien and Menon 1995; Chien et al. 2011; Bolan et al. 1990). For example, McLean and Logan (1970) indicated that even soluble P fertilizers have low agronomic efficiency in soils with high P-fixing capacity.

AMW-Induced Changes in Phosphorus Speciation

XRD and XANES analyses provided complementary, direct evidence for mineral alterations induced by AMW treatments of PRs. Diffraction showed a dominance of apatite in the original samples (0% AMW treatment) for all three PRs (Fig. 2). The diffraction peaks for the Bayóvar PR sample were broader than those for the Araxá and Patos PRs, indicating that Bayóvar PR contained more poorly crystalline apatite. Consistent with XRD results, P K-edge XANES spectra for the original PR showed a post-edge shoulder near 2154 eV (arrow in Fig. 3) and a broad peak near 2162 eV. These peaks are indicative of hydroxyapatite (Hesterberg et al. 1999).

The intensity of XRD peaks for hydroxyapatite, e.g., at 30, 37-40, 55, and 58° 2θ, progressively diminished with increasing AMW concentration (Fig. 3). The broader peaks for Bayóvar PR essentially disappeared in the 25% AMW treatment, and the sharper peaks for Araxá and Patos PRs were detected up to at least the 50% treatment. Following the breakdown of hydroxyapatite structure, gypsum (CaSO₄·2H₂O) was formed from all PRs. The Patos PR treated with 75% AMW also contained anhydrite (CaSO₄), probably due to gypsum dehydration during drying (Fig. 3). XRD patterns also showed that minor amounts of quartz persisted in the Patos PR following all AMW treatments.

Qualitative changes in P K-edge XANES spectra showed a progressive transformation of apatite in PRs into new P species. A loss of apatite with increasing AMW treatment concentration is apparent from the decreasing prominence of both the post-white

line shoulder near 2154 eV (arrow in Fig. 3) and the broad peak near 2162 eV, consistent with XRD data. Although the shape of the shoulder at 2154 eV varies between different Ca-phosphate minerals, hydroxyapatite shows the most prominent shoulder (*Beauchemin et al.* 2003; *Hesterberg et al.* 1999; *Ingall et al.* 2010; *Lombi et al.* 2006; *Toor et al.* 2006). Concurrent with a loss of hydroxyapatite, the progressive formation of a weak pre-white line peak between ~2146 and 2149 eV (arrow and inset in Fig. 3) with increasing AMW concentration indicated that the AMW treatments induced the formation of Fe(III)-bonded phosphate (*Franke and Hormes* 1995; *Hesterberg et al.* 1999; *Khare et al.* 2005; *Okude et al.* 1999) assigned this peak to a P 1s electron transition into Fe(4p)-O(2s) antibonding molecular orbitals and indicated that the peak intensity is related to the number of PO₄-Fe(III) bonds in the species. Consequently, the intensity of the pre-edge peak is greater for strengite than for less crystalline Fe(III)-phosphates. Iron phosphate was not detectable by XRD, suggesting that it was either amorphous or at a concentration below detection.

Quantitative assessments of P speciation changes are shown by linear combination fitting results (Table 4). The two fitting approaches that we used were intended to evaluate the consistency of our fitting models, i.e., fitting the 12.5% and 25% AMW-treatment samples with endmembers of 0% and 75% AMW treatments (“fit with endmembers”) or fitting with combinations of up to four standards (“fit with standards”). Although better fits were obtained with standards as indicated by the typically lower residual (R-factor) for a given sample (Table 4) and the excellent agreement between sample data and fits (Fig. 3), the fits with endmembers indicated that there was a progressive decrease in the starting materials (PRs) and a progressive increase in the ending materials (75% treatment samples) with increasing AMW concentration (Table 4). Results of fitting with standards were generally consistent with this progressive trend. The proportion of the original PR in the fits progressively decreased with increasing AMW concentration, and the proportion of Fe (III)-bonded phosphate increasing. The Fe(III)-bonded phosphate was best fit with a standard of “FePO₄·2H₂O” from Sigma-Aldrich (CAS 13463-10-0), which was verified by XRD analysis to be non crystalline, rather than with the poorly crystalline or well crystalline strengite standards published by *Hesterberg et al.* (1999). The progressive formation of up to 78%, 38%, and 70% of P as amorphous Fe(III)-phosphate in the AMW-treated samples of Araxá, Patos, and Bayóvar PRs samples, respectively, was consistent with the lack of

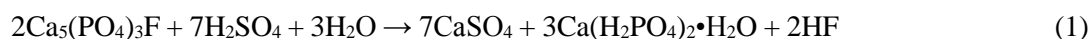
detectable peaks for Fe(III)-phosphate minerals in our XRD patterns (Table 4, Fig. 2). Based on Fe and P concentrations in Tables 1 and 2, and a mass balance analysis given our reaction conditions, molar ratios of Fe/P in the reacted PR and AMW samples indicate that the maximum proportions of amorphous FePO₄ that could form in the 75% AMW treatments are 32, 19, and 29% of total P for the Araxá, Patos, and Bayóvar PR samples, respectively. These results indicate that our XANES fitting analysis overestimated the proportion of P present as FePO₄. However, it is probable that the methodology described by *Alcarde* (2009) to extract total P concentration from PRs underestimates Fe concentration.

In addition to the loss of PR apatite and the apparent formation of amorphous Fe(III)-phosphate, linear combination fitting results indicated the formation of other Ca-phosphate species following AMW treatments. These species were fit with an amorphous Ca-phosphate standard- published by *Eveborn et al.* (2009)-, a monocalcium phosphate (MCP) standard [Ca(H₂PO₄)₂ purchased from Vetec Química Fina Ltda], or a dicalcium phosphate (DCP) standard (CaHPO₄ purchased from same Company) (Table 4). The tendency was for a species fit with monocalcium phosphate to be formed in the 12.5% and 25% AMW samples, with species fit with amorphous Ca-phosphate and dicalcium phosphate standards becoming progressively greater with increasing AMW concentrations. Although the fits included up to 30% of total P as MCP or DCP, the overall concentration of these minerals (for PRs containing 30% P₂O₅) would be ≤10% (w w⁻¹) and were not detected by XRD analysis.

In the Patos sample treated with 12.5% AMW, the best fit included 7% of total P represented by an amorphous Al-phosphate standard (Table 4). Perhaps at this lowest acid treatment, Al³⁺ was preferentially dissolved over Fe³⁺ in this sample of greatest Al/Fe ratio (Table 1) and amorphous Al-phosphate formed in preference to amorphous Fe-phosphate. Because fits with species at concentrations of <10% of total P are considered minor species near the limit of sensitivity of P K-edge XANES analysis, conclusions about their mechanisms of formation and their overall contribution to the reactivity of the AMW-treated PR samples are tentative.

Discussion

Treatment of Araxá, Patos, and Bayóvar PRs with AMW increased the fertilizer value of the material as indicated by the increasing extractable amounts of P (P_{water} , P_{NAC} and P_{CA}). The AMW-induced changes were somewhat consistent with those induced by reaction of PRs with pure acids such as sulfuric acid in the production of simple superphosphate (SSP) fertilizer (*Leikam and Achorn 2005*), e.g.,



XRD and XANES results both showed a loss of apatite with increasing AMW concentration between 12.5 and 75% (v v^{-1}), and XRD also showed formation of gypsum and anhydrite (Figs. 2 and 3; Table 4). Moreover, XANES spectral fitting also indicated a progressive formation of amorphous Fe-phosphate (Table 4), apparently induced by high concentrations of Fe in the AMW (13595 mg/L or 0.24 mol/L – Table 2) and the PRs (9100 – 44000 mg/kg; Table 1). Although our XRD patterns showed no evidence for formation of SSP [$\text{Ca}(\text{H}_2\text{PO}_4)_2 \cdot \text{H}_2\text{O}$] according to reaction (1), XANES fitting results suggested that apatite was converted to more soluble Ca-phosphate species that were fit as amorphous Ca-phosphate, MCP, and DCP. Linear increases in P_{water} , P_{NAC} , and P_{CA} with increasing AMW concentration for the Araxá and Bayóvar PRs (Fig. 1) indicate that the greatest fertilizer value can be achieved with maximum AMW treatment for these PRs. Thus, we recommend an AMW treatment of 75% for these PRs in any commercialization process to maximize P solubility and also the consumption of AMW that would otherwise contribute to the waste stream of the Ta and Nb oxides production process. For the Patos PR, derivatives of quadratic relationships between P_{water} and P_{CA} with respect to AMW concentration (Fig. 1) showed maxima at 45% and 62%, respectively. We recommend an AMW treatment of 50% in any commercialized processing of Patos PR.

The effect of the AMW treatment on soluble P can be better understood by considering changes in P speciation. Fig. 4 shows a significant negative linear relationship between P_{NAC} and the proportion of total P fit as hydroxyapatite from XANES spectra, and corresponding positive linear relationships between P_{NAC} and fitted proportions amorphous Ca-phosphate, DCP, and amorphous Fe-phosphate fit from the XANES spectra. Note that we forced the regressions for the Ca- and Fe-phosphate lines to the origin to make a more

direct comparison of slopes. The relationships in Fig. 4 imply that conversion of apatite to other P forms following AMW treatments is key to increasing the solubility in of P in the PR samples. The greater positive slopes for the Ca-phosphates compared with the amorphous Fe-phosphate suggest that the species fit as amorphous Ca-phosphate and DCP were more soluble, and both species showed identical linear relationships when regressions are forced to the origin. Although the proportion of the species fit as MCP showed no significant relationship with P_{NAC} , we expect this Ca-phosphate species to be more soluble than hydroxyapatite. Moreover, P_{CA} and P_{water} showed similar trends as P_{NAC} with XANES species, but generally had higher p values.

In summary, the AMW treatment causes speciation changes that should enhance the fertilizer quality of PRs based on common extractions used to evaluate plant-available P concentrations. However, because commercial fertilizers produced using pure acids apparently contain phosphate only in soluble Ca-phosphate species (e.g., SSP, TSP), evaluations of the AMW-treated PRs in soils are needed to determine, for example, the plant availability of the amorphous Fe-phosphate species in a soil matrix in which pH and interactions with Fe-oxides and organic matter should affect Fe-phosphate dissolution.

One potential concern with using AMW to improve the fertilizer quality of PRs is the addition of potentially toxic trace elements to the resulting fertilizer product. Mass balance calculations on the additions of trace elements relative to the native concentrations for the various PR sources and AMW treatments showed that the fertilizer products would be enriched in trace elements by up to 126-fold for the 75% AMW treatment. Trace-element enrichment in all three fertilizers generally followed the order $Cd > Ni > Mn > Cu > Cr > Pb > Zn$. The greatest enrichment occurred for the Patos PR, mainly because it contained the lowest native concentrations of trace elements. However, for all PR sources and AMW treatments, the concentrations of As, Cd, Pb, Cr, and Hg in the AMW-treated byproducts never exceeded the maximum allowable concentrations of 2, 4, 20, 40, and 0.05 mg/kg, respectively, per percentage (1% w w⁻¹) of P₂O₅ content, according to standards adopted in Brazil for phosphate fertilizers. The maximum computed concentrations (assuming 100% incorporation of trace elements added with AMW 75%) were 2279, 235, 151, 138, 91, 84 and 26 mg kg⁻¹ for Mn, Ni, Zn, Cr, Pb, Cu and Cd, respectively (data not shown).

Except for the Bayóvar PR, our AMW treatments produced lower concentrations of P_{water} and P_{NAC} than are found for commercial phosphate fertilizers such as SSP and TSP, (Table 3). However, some poor-quality SSP sources may contain as little as 50–60% water soluble P (Chien *et al.* 2011). Although high concentrations of water-soluble P can be a quality index for phosphate fertilizer, several papers show that partially acidulated PRs can be more effective for slower release of P (Chien and Hammond 1988; McLay *et al.* 2000; Prochnow *et al.* 2006; Prochnow *et al.* 2002) than more water soluble superphosphate fertilizers. Because Bayóvar is considered the highest-quality of the three PRs that we evaluated, it might be better to develop high grade fertilizers from Bayóvar PR using pure acids to avoid the introduction of trace-element impurities from AMW treatment. Also, the Bayóvar PR can be used directly for perennial crops without acidification. Nevertheless, by consuming 100% of the 17,250 m³ of AIW produced by the mining industry each year, and considering the best AMW concentrations that we found to solubilize Araxá or Bayóvar PRs (75%) or Patos PR (50%), it is possible to produce 15,000 or 22,600 metric tons of P fertilizer, respectively.

Conclusions

Reacting PRs with AMW appears to be a viable alternative for using pure acids to produce high-grade phosphate fertilizers. Production with AMW eliminates the cost of the pure acids and has an added environmental benefit of consuming a hazardous acid waste from a mining industry. Our AMW treatments increased phosphate extractable in water (P_{water}), neutral ammonium citrate (P_{NAC}), and citric acid (P_{AC}) by approximately 300-, 30- and 3-fold, respectively. Complementary XRD and P K-edge XANES analyses indicated that the increased solubility of P was due to conversion of apatite to more soluble phosphates, including amorphous iron (III) phosphate and possibly amorphous Ca-phosphate, dicalcium phosphate (DCP), or monocalcium phosphate (MCP). Our speciation analysis would also be valuable for understanding the fate of fertilizer products from AMW treatment when applied to soils.

Acknowledgements

This research was carried out at the National Synchrotron Light Source (LNLS), Campinas-SP, Brazil. The authors are thankful to the London Scandinavian Metal Brasil S.A (UFV no 50230261299) for funding this research. We are also thankful to the Brazilian agency CAPES (Coordination for the Improvement of Higher Education Personnel – project CAPES-A105/2013) for providing funding for the participation of Dean Hesterberg in this project (visiting researcher), a PhD scholarship for Wedisson Oliveira Santos at NC State University. We are grateful to Dr. David Eveborn for providing a XANES spectrum for the amorphous Ca-phosphate standard used in this study.

References

- Alcarde JC (2009) Manual de análise de fertilizantes vol 1. FEALQ, Piracicaba, Brasil. 259 p.
- Beauchemin S, Hesterberg D, Chou J, Beauchemin M, Simard RR, Sayers DE (2003) Speciation of phosphorus in phosphorus-enriched agricultural soils using X-ray absorption near-edge structure spectroscopy and chemical fractionation. *J Environ Qual* 32:1809-1819
- Beisiegel WR, de Souza WO (1986) Reservas de fosfatos--Panorama nacional e mundial. Instituto Brasileiro de Fosfato (IBRAFOS) III Encontro Nacional de Rocha Fosfática, Brasília:16-18
- Bolan NS, Hedley MJ, Harrison R, Braithwaite AC (1990) Influence of manufacturing variables on characteristic and the agronomic value of partially acidulated phosphate fertilizers. *Ferti Res* 26:119-138
- BRASIL (2011) Resolução n 430 de 13 de maio de 2011. Dispõe sobre as condições e padrões de lançamento de efluentes, complementa e altera a Resolução. Available at: <http://www.mma.gov.br/port/conama/res/res11/res43011.pdf>.
- Capón-García E, Papadokostantakis S, Hungerbühler K (2014) Multi-objective optimization of industrial waste management in chemical sites coupled with heat integration issues. *Comput Chem Eng* 62:21-36

- Chien SH, Carmona G, Henao J, Prochnow LI (2003) Evaluation of rape response to different sources of phosphate rock in an alkaline soil. *Commun Soil Sci Plan* 34:1825-1835
- Chien SH, Hammond LL (1988) Agronomic evaluation of partially acidulated phosphate rocks in the tropics: IFDC's experience. International Fertilizer Development Center.
- Chien SH, Menon RG (1995) Factors affecting the agronomic effectiveness of phosphate rock for direct application. *Ferti Res* 41:227-234
- Chien SH, Prochnow LI, Tu S, Snyder CS (2011) Agronomic and environmental aspects of phosphate fertilizers varying in source and solubility: an update review. *Nutr Cycl Agroecosys* 89:229-255
- Cordell D, Rosemarin A, Schröder JJ, Smit AL (2011) Towards global phosphorus security: A systems framework for phosphorus recovery and reuse options. *Chemosphere* 84:747-758
- Diaz J, Ingall E, Benitez-Nelson C, Paterson D, de Jonge MD, McNulty I, Brandes JA (2008) Marine polyphosphate: a key player in geologic phosphorus sequestration. *Science* 320:652-655
- Dorozhkin SV (1997) Acidic dissolution mechanism of natural fluorapatite. II. Nanolevel of investigations. *J Cryst Growth* 182:133-140
- Dorozhkin SV (1999) Inorganic chemistry of the dissolution phenomenon: the dissolution mechanism of calcium apatites at the atomic (ionic) level. *Comments Inorg Chem* 20:285-299
- Dorozhkin SV (2012) Dissolution mechanism of calcium apatites in acids: A review of literature. *World J Methodol* 2:1-17
- Eveborn D, Gustafsson JP, Hesterberg D, Hillier S (2009) XANES speciation of P in environmental samples: An assessment of filter media for on-site wastewater treatment. *Environ Sci Technol* 43:6515-6521
- Faria FM, Guardieiro GA (2011) Adubação fosfatada na cultura da soja. *Revista Passarela da Soja*:105-111
- Franke R, Hormes J (1995) The P K-edge absorption spectra of phosphates. *Physica B: Condensed Matter* 216:85-95

- Hesterberg D, Zhou W, Hutchison KJ, Beauchemin S, Sayers DE (1999) XAFS study of adsorbed and mineral forms of phosphate. *J Synchrotron Radiat* 6:636-638
- Ingall ED et al. (2010) Phosphorus K-edge XANES spectroscopy of mineral standards. *J Synchrotron Radiat* 18:189-197
- Kar G, Peak D, Schoenau JJ (2012) Spatial distribution and chemical speciation of soil phosphorus in a band application. *Soil Sci Soc Am J* 76:2297-2306
- Kelly SD, Hesterberg D, Ravel B (2008) Analysis of soils and minerals using X-ray absorption spectroscopy. *Methods of soil analysis Part 5*:387-463
- Khare N, Hesterberg D, Martin JD (2005) XANES investigation of phosphate sorption in single and binary systems of iron and aluminum oxide minerals. *Environ Sci Technol* 39:2152-2160
- Khaliq R, Hettiarachchi GM, Mengel DB, Fei M (2012) Speciation of phosphorus in a fertilized, reduced-till soil system: In-field treatment incubation study. *Soil Sci Soc Am J* 76:2006-2018
- Kizewski F, Liu Y-T, Morris A, Hesterberg D (2011) Spectroscopic approaches for phosphorus speciation in soils and other environmental systems. *J Environ Qual* 40:751-766
- Lapido-Loureiro FEV, Melamed R (2006) O fósforo na agricultura brasileira: uma abordagem minero-metalúrgica. *Centro de Tecnologia Mineral: Rio de Janeiro*
- Lehr JR (1980) Phosphate raw materials and fertilizers: Part I—A look ahead. The role of phosphorus in agriculture:81-120
- Lehr JR (1984) Impact of phosphate rock quality on fertilizer market uses. *Industry and Mineralogy* 200:127-153
- Leikam DF, Achorn FP (2005) Phosphate fertilizers: Production, characteristics, and technologies. *Agron J* 46:23
- Lombi E, Scheckel KG, Armstrong RD, Forrester S, Cutler JN, Paterson D (2006) Speciation and distribution of phosphorus in a fertilized Soil. *Soil Sci Soc Am J* 70:2038-2048
- Manceau A, Nagy KL (2012) Quantitative analysis of sulfur functional groups in natural organic matter by XANES spectroscopy. *Geochim Cosmochim Acta* 99:206-223
- Mattiello EM et al. (2015) Soluble phosphate fertilizer production using acid effluent from metallurgical industry. *J Environ Manage* 166:140-146

- McLay CDA, Rajan SSS, Liu Q (2000) Agronomic effectiveness of partially acidulated phosphate rock fertilizers in an allophanic soil at near-neutral pH. *Commun Soil Sci Plan* 31:423-435
- McLean EO, Logan TJ (1970) Sources of phosphorus for plants grown in soils with differing phosphorus fixation tendencies. *Soil Sci Soc Am J* 34:907-911
- Nriagu JO, Moore PB (1984) *Phosphate minerals*. Springer-Verlag. 442 p.
- Oba CAI (2004) *Fabricação de um fertilizante organo-fosfatado*. Rio de Janeiro: CETEM/MCT
- Okude N, Nagoshi M, Noro H, Baba Y, Yamamoto H, Sasaki TA (1999) P and S K-edge XANES of transition-metal phosphates and sulfates. *J Electron Spectrosc* 101: 607-610
- Prietzl J, Dümig A, Wu Y, Zhou J, Klysubun W (2013) Synchrotron-based P K-edge XANES spectroscopy reveals rapid changes of phosphorus speciation in the topsoil of two glacier foreland chronosequences. *Geochim Cosmochim Acta* 108:154-171
- Prochnow LI, Chien SH, Carmona G, Austin ER, Corrente JE, Reynaldo FAL (2006) Agronomic effectiveness of cationic phosphate impurities present in superphosphate fertilizers as affected by soil pH. *Commun Soil Sci Plan* 37:2057-2067
- Prochnow LI, Chien SH, Carmona G, Henao J (2004) Greenhouse evaluation of phosphorus sources produced from a low-reactive Brazilian phosphate rock. *Agron J* 96:761-768
- Prochnow LI, van Raij B, Kiehl JC (2002) Effect of water and citrate solubility on agronomic effectiveness of acidulated phosphates in three consecutive corn crops. *R Bras Ci Solo* 26:729-736
- Puig R, Fullana-i-Palmer P, Baquero G, Riba J-R, Bala A (2013) A Cumulative Energy Demand indicator (CED), life cycle based, for industrial waste management decision making. *Waste Manage* 33:2789-2797
- Ravel B, Newville M (2005) ATHENA, ARTEMIS, HEPHAESTUS: data analysis for X-ray absorption spectroscopy using IFEFFIT. *J Synchrotron Radiat* 12:537-541
- Sato S, Solomon D, Hyland C, Ketterings QM, Lehmann J (2005) Phosphorus speciation in manure and manure-amended soils using XANES spectroscopy. *Environ Sci Technol* 39:7485-7491

- Silva IR, Smyth TJ, Raper CD, Carter TE, Rufty TW (2001) Differential aluminum tolerance in soybean: an evaluation of the role of organic acids. *Physiol Plantarum* 112:200-210
- Teixeira AO et al. (2005) Chemical composition of different phosphorus sources and heavy metal deposition in tissues of swines. *Arq Bras Med Vet* 57:502-509
- Toor GS, Hunger S, Peak JD, Sims JT, Sparks DL (2006) Advances in the characterization of phosphorus in organic wastes: Environmental and agronomic applications. *Adv Agron* 89:1-72
- Wright R, Stuczynski T (1996) Atomic absorption and flame emission spectrometry. In: al. SDe (ed) *Methods of Soil Analysis. Part 3- Chemical Methods*, vol 29. SSSA, Madison, WI, pp 65-90
- Young R (1974) Implications of atomic substitutions and other structural details in apatites. *J Dent Res* 53:193-203

Table 1 Chemical composition of Araxá, Patos and Bayóvar phosphate rocks

NPs	P ₂ O ₅	Fe ₂ O ₃	Al ₂ O ₃	MnO	Zn	Ni	Pb	Cu	Cr	Cd
-----(% w w ⁻¹)-----					-----mg/kg-----					
Araxá	30	6.3	0.83	0.22	264	69	52	50	37	1.1
Patos	30	1.3	1.45	0.014	63	5.5	29	22	16	0.1
Bayóvar	29	5.1	1.49	0.31	181	239	70	23	186	36

Table 2 Chemical composition of acidic mining waste (AMW) from London Scandinavian Metal Brasil S.A.

Density	pH	acidity†	Fe	K	Mn	Al	Ni	Cr	Cu
(kg/m ³)		(mol/L)	-----mg/L-----						
1.6	0.0	5.8	13595	3438	1199	897	126	59	57
Pb	Ca	Zn	Cd	Mg	SO ₄ ²⁻	Cl ⁻	F ⁻	PO ₄ ³⁻	NO ₃ ⁻
-----mg/L-----					-----g/L-----				
56	46	44	11	4.7	791	128	109	19	18

†Acid buffering measured by neutralization of AMW to pH 7 with 0.5 mol/L of NaOH.

Table 3 Percentages of water- (P_{water}), neutral ammonium citrate (P_{NAC}), and citric acid (P_{CA}) soluble P_2O_5 contents of phosphate rocks (PRs) reacted with acidic mining waste (AMW) increased with increasing waste concentration

AMW (% v v ⁻¹)	Araxá Phosphate			Patos Phosphate			Bayóvar Phosphate		
	P_{water}	P_{NAC}	P_{CA}	P_{water}	P_{NAC}	P_{CA}	P_{water}	P_{NAC}	P_{CA}
	(P_2O_5 , % w w ⁻¹ of total P)								
0	0.1±0.1	2.3±0.8	15.2±0.4	0.03±0.0	2.2±1.4	21.8±2.1	0.7±0.1	2.4±0.8	35.8±2.7
12.5	3.5±0.2	10.6±2.5	15.1±1.2	3.5±2.5	10.1±0.3	24.4±1.0	11.8±2.1	10.9±2.3	27.6±1.9
25	9.6±0.6	29.1±6.3	25.2±4.9	28.8±0.7	37.2±1.5	45.1±4.6	16.2±0.9	26.6±4.8	45.1±6.1
50	16.4±7.4	36.5±9.1	22.1±5.4	26.0±6.3	42.2±1.4	42.4±7.9	42.7±7.2	53.1±6.2	48.6±9.0
75	25.2±5.9	60.7±7.2	49.8±2.6	15.8±4.6	45.4±2.3	37.2±5.3	76.0±4.1	99.8±3.4	90.5±4.2

Table 4. Best-fit proportions of standards (\pm uncertainties) from two approaches to LCF fitting of P K-edge XANES spectra of PRs for the different AMW treatments: (1) fitting of the 12.5 and 25% AMW samples using the original PR (0%) and 75% AMW samples as “endmember” treatment standards; and (2) fitting with the original PR and standards of amorphous iron (III) phosphate (Am-FePO₄), amorphous calcium phosphate (Am-Ca-P), monocalcium phosphate [MCP, Ca(H₂PO₄)₂], dicalcium phosphate [DCP, CaHPO₄], and amorphous aluminum phosphate (Am-AlPO₄).[†]

		Fit with endmembers		Fit with Standards						R-Factor x 10 ⁻⁴ ‡
		Original RP	75% AMW	Original RP	Am-FePO ₄	Am-Ca-P	MCP	DCP	Am-AlPO ₄	
		----- % of total P -----								
Araxá	12.5	70 ± 1	30 ± 1	59 ± 1	19 ± 0		22 ± 1			14, 4
	25	48 ± 1	52 ± 1	33 ± 2	37 ± 0	17 ± 2	13 ± 1			8, 4
	75				78 ± 1	22 ± 1				14
Patos	12.5	73 ± 2	27 ± 2	74 ± 2			12 ± 2	7 ± 2	7 ± 2	20, 13
	25	27 ± 1	73 ± 1	43 ± 2	25 ± 1	13 ± 2		19 ± 2		3, 3
	75			27 ± 2	38 ± 1	14 ± 2		22 ± 2		4
Bayóvar	12.5	89 ± 0	11 ± 0	85 ± 1	8 ± 0	3 ± 2	4 ± 1			3, 2
	25	71 ± 1	29 ± 1	62 ± 1	19 ± 0		19 ± 1			19, 3
	75				70 ± 1			30 ± 1		16

[†]Fitted proportions of standards all summed to between 96 and 104% and were re-normalized to a sum of 100%. Uncertainties calculated by Athena were rounded to the nearest whole number. Percentages of standards <5% of total P are considered to be at “trace” levels relative to the sensitivity of XANES analysis. [‡]R-factor = $\sum(\text{data-fit})^2/\sum(\text{data})^2$, is a measure of the residual in the fit. The first of two numbers for 12.5 and 25% treatments is for fits with endmembers.

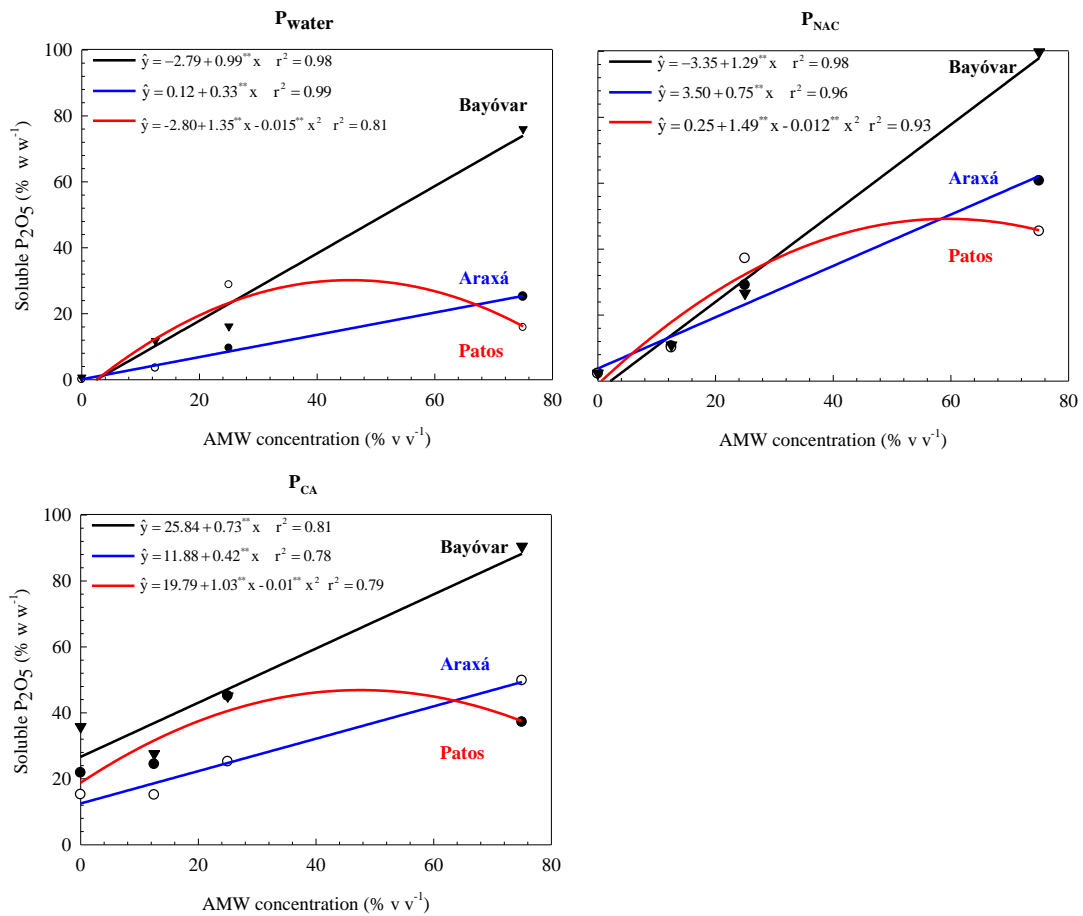


Fig.1 Percentages of water- (P_{water}), neutral ammonium citrate (P_{NAC}), and citric acid (P_{CA}) soluble P_2O_5 in phosphate rocks reacted with acidic mining waste (AMW) generally increased with increasing AMW concentration. Linear or quadratic regression relationships between soluble P_2O_5 and AMW concentration were significant at either the 95% ($p = 0.05$, “*”) or 99% ($p = 0.01$, “**”) levels, except for P_{CA} for the Patos rock phosphate.

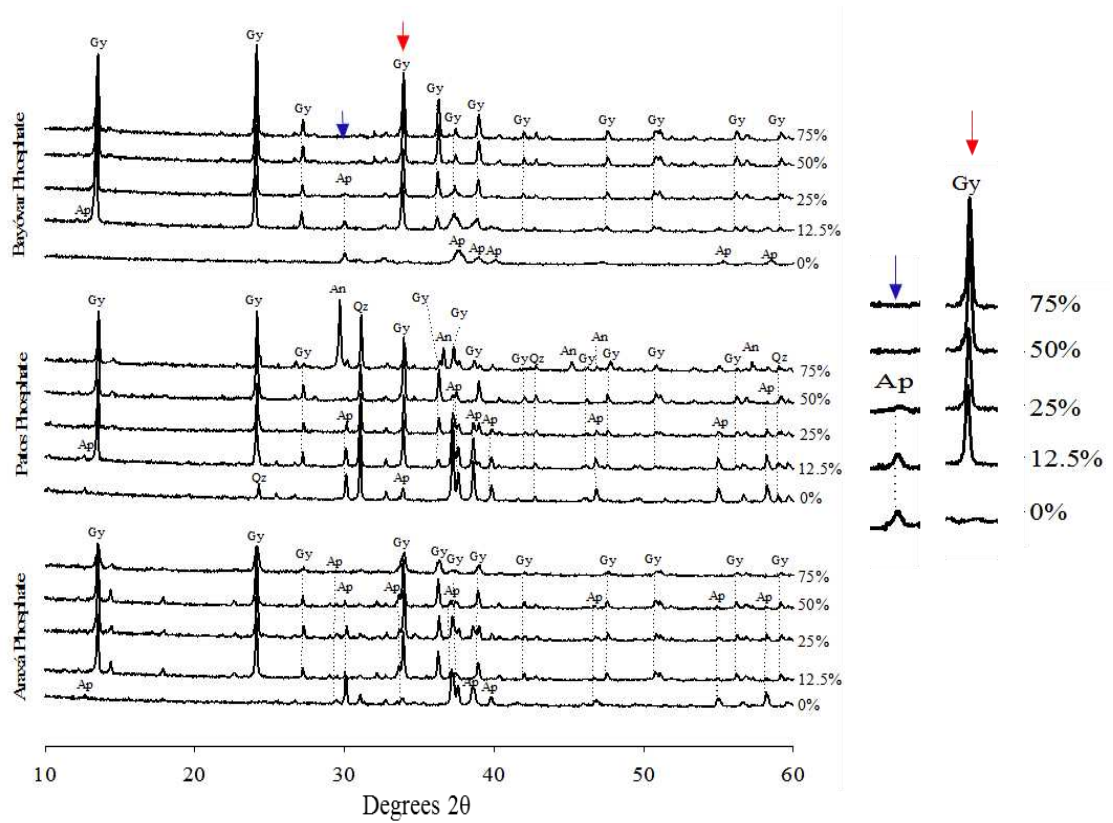


Fig. 2 X-ray diffraction (XRD) patterns from phosphate rocks (Araxá, Patos and Bayóvar) following treatment with different concentrations of acidic mining waste (AMW): 0, 12.5, 25, 50, or 75% (v v⁻¹). Gy-gypsum, An-anhydrite, Ap-apatite, Qz-quartz. X-ray diffraction shows the disappearance of apatite and the appearance of gypsum (CaSO₄•2H₂O) or anhydrite (CaSO₄) with increasing AMW concentration. Quartz (Qz) is present to all the AMW treatments using Patos PR. Data were collected using Co K_{α1} radiation (1.789 Å).

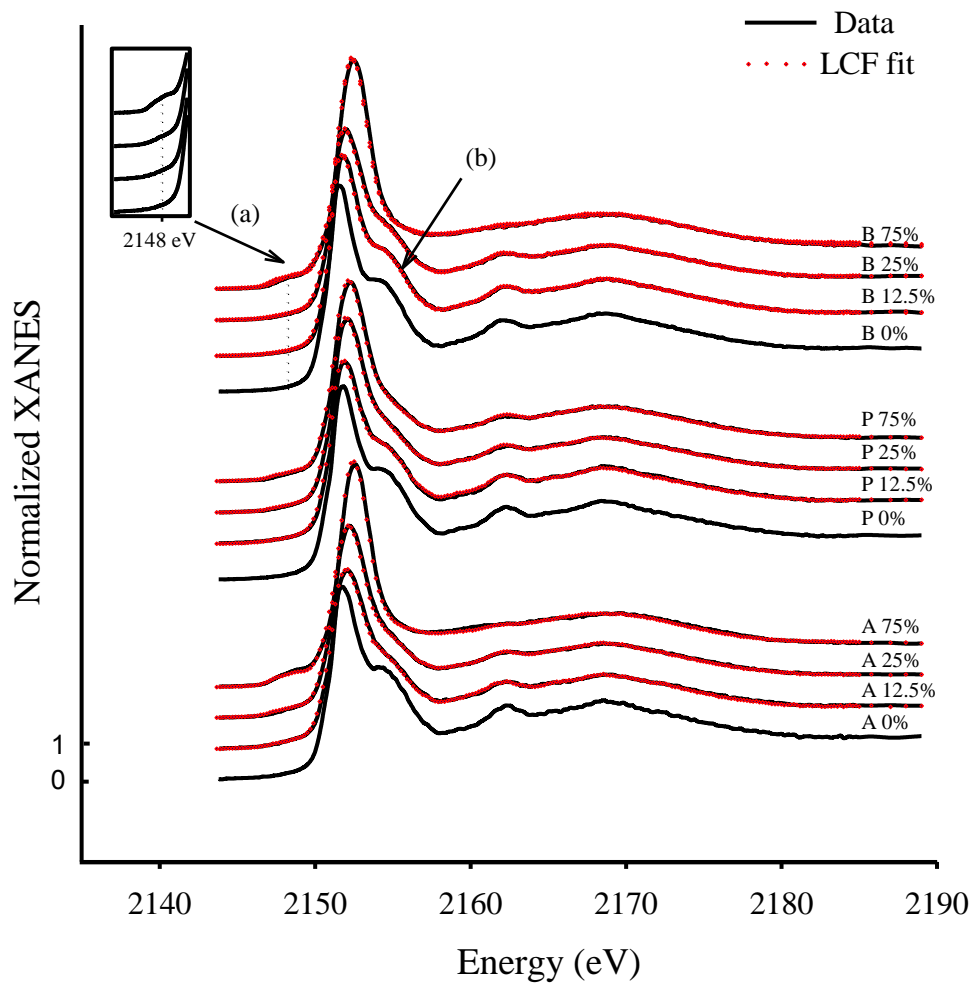


Fig. 3 Spectra show changes in P speciation with increasing concentration of reacted AMW, including a disappearance of apatite as indicated by the weakening of a shoulder near 2155 eV (arrow *b*) across treatments, and the appearance of Fe (III)-bonded phosphate as indicated by a growth in a pre-white line feature near 2148 eV (arrow *a*).

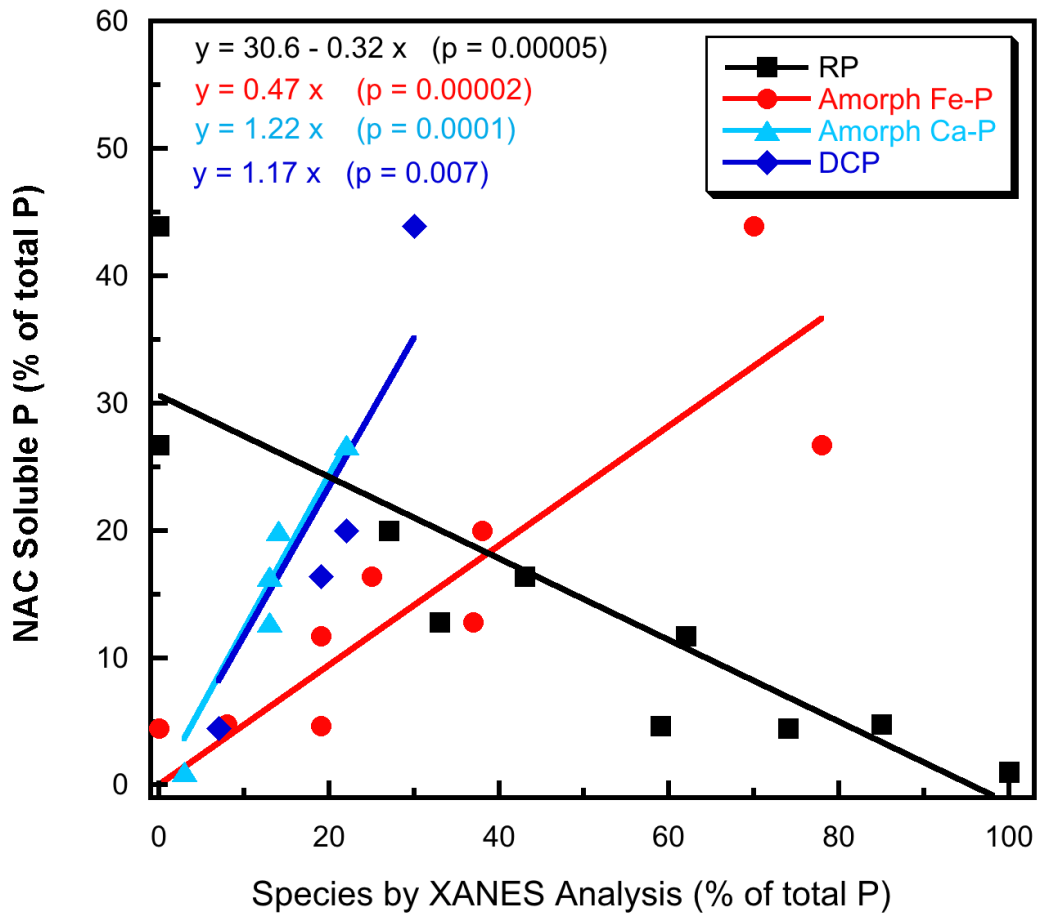


Fig. 4 Linear relationships between neutral ammonium citrate (P_{NAC}) soluble P and proportions of selected P species fit to phosphorus K-edge XANES spectra (Table 4) for all three phosphate rocks (PRs) treated with all concentrations of acidic mining waste (AMW). Fits for water (P_{water}) and citric-acid (P_{CA}) soluble P (not shown) gave similar trends.

ARTIGO 3

Production and evaluation of potassium fertilizers from silicate rock

Wedisson Oliveira Santos*¹, Edson Marcio Mattiello¹, Leonardus Vergutz¹, Rodolfo Fagundes Costa¹

¹Department of Soil Science, Universidade Federal de Viçosa (UFV), Av P H Rolfs, Viçosa, Minas Gerais, Brazil, CEP 36570-000

Abstract

Rising price and limited geographical availability of traditional sources of potassium (K) fertilizers have stimulated a search for alternative K sources in different parts of the world. In this research, we evaluated mineral transformations and agronomic properties of an alternative source of K produced through thermal and chemical treatment of the verdetite rock. Chemical and mineralogical characteristics were evaluated before and after each treatment. Four K sources (verdetite rock, KCl, acidified verdetite and calcinated verdetite) were applied to an Oxisol soil at different rates. Eucalyptus and sequentially cropped maize and grass were grown in the treated soils. Verdetite rock has very low solubility in water and in citric acid and its mineralogical composition is glauconite and microcline as K minerals. Thermal and chemical treatments increased the concentration of water soluble K and citric acid soluble K. These treatments also caused crystalline K minerals to collapse and form sylvite and arcanite. Verdetite rock was not suitable as a K source for maize and eucalypt. Fertilizers from thermal or chemical treatments showed agronomic performance similar to KCl. When K was applied as K-calcinated verdetite, 82% of the total K was recovered in maize and grass cultivations. Less K was recovered in plant following addition of K-acidified verdetite and KCl (72% and 77%, respectively). Potassium recoveries by eucalypt were about 52, 53 and 60% of amount applied of

calcined verdete, acidified verdete and KCl, respectively. The K sources that were produced following calcination and thermal treatment were equivalent to that provided by KCl.

Key words: Alternative / Glaucconitic rock / Sources of potash / Verdete

1 Introduction

Potassium is a vegetal nutrient generally found in low concentrations in tropical soils. Due to the high demand of K for cultivation, this nutrient is required in large amounts in crop fertilization schemes. On the other hand, few countries in the world are self-sufficient in the production of K fertilizers. This is due to the limited natural occurrence of soluble K minerals such as sylvite (KCl), sylvinite (KCl+NaCl), carnalite (KMgCl₃.6H₂O) and langbeinite [(K₂Mg₂(SO₄)₃)]. Potassium ore reserves are found mostly in the Northern Hemisphere, specifically, in Canada, Russia, Belarus and Germany. Together, these countries are responsible for approximately 85% of the K market worldwide (*Lima and Neves, 2012; Ott, 2012*).

Potassium fertilizer consumption continues to increase every year. Thus, due to future uncertainties about the market supply of K fertilizers, countries as Brazil, China and India have directed their research to exploitation of domestic sources of K from silicates ores (*Eichler, 1983; Varadachari, 1992; Yadav and Sharma, 1992; Mazumder et al., 1993; Nascimento, 2004b; Loureiro et al., 2010; Toledo Piza et al., 2011; Santos et al., 2015*). These investigations have showed that there is an abundance of K minerals, such as micas and feldspars, in all of these countries. However, these minerals have very low water solubility and as such, their effectiveness as a fertilizer for plant growth has been questioned (*Blum et al., 1989; Coroneos et al., 1995; Ramezani et al., 2013*).

Increasing the water-solubility of K in these minerals has been investigated previously using chemical and thermal treatments (*Eichler, 1983; Nascimento, 2004a; Santos et al., 2015*).

In Brazil, one of the most abundant K silicate minerals is verdete. The total reserve of this rock in Brazil is unknown, however, the municipality of Cedro do Abaeté, is known to have reasonable reserves of verdete (57.4 million tons) (*Alecrim, 1982*). Verdete is a glauconitic metasedimentary rock with a K₂O concentration of approximately of 7% (w w⁻¹) (*Silva et al., 2012; Toledo Piza et al., 2011*).

Although several studies have investigated the effects of chemical and thermal treatments on potassium silicate rock (*Eichler, 1983; Mazumder et al., 1993; Valarelli et al., 1993; Nascimento, 2004a; Toledo Piza et al., 2011; Santos et al., 2015*), the availability of K in these products to crops remains unclear.

Our goal is to develop an alternative potassium fertilizers produced by reacting of potassium rock (verdete) with acid industrial effluent (AIE) and thermal process using CaCl₂.2H₂O as fluxing agent. The specific objective of this research was to analyze transformation products and the extractability of K in water and citric acid in materials produced by reacting chemical and thermal with verdete. Measurements of K extractability by reagents used to evaluate fertilizer quality, bulk mineralogy, and agronomic parameters using maize, grass and eucalyptus as test plants were made.

2 Materials and methods

2.1 Rock sampling and preparation

A representative sample of 10 kg of verdete rock was collect in Cedro do Abaeté, in Minas Gerais State, Brazil. Geologically, verdete rock occurs in the Bambuí formation on the Serra da Saudade in the São Francisco Craton (*Valarelli et al., 1993*). Prior to chemical and mineralogical analyses, rock samples were ground and passed through a

75- μm sieve (200 mesh). Before thermal and chemical treatment, rock was passed through a larger sieve (150 μm).

2.2 Acidified Verdete

In order to produce the acidified verdete we used an acid industrial effluent (AIE), collected from the LSM (London & Scandinavian Metallurgical Brasil S.A), located in São João Del Rei, Minas Gerais State, Brazil. This effluent is the by-product of tantalum (Ta) and niobium (Nb) production from pegmatite and uses a three-acid ($\text{H}_2\text{SO}_4/\text{HF}/\text{HCl}$) leaching process. The annual production of AIE is around 22,800 m^3 , which after alkaline neutralization results in 12,700 Mg of mud (Personal information from LSM). The AIE had a very low pH (~ 0) and concentrations of cations and anions were above those permitted by national legal limits (*BRASIL*, 2001) for disposal into a receiving watercourse (Table 1). The AIE was used to increase verdete reactivity and to potentially produce soluble K minerals at a low cost by reusing this industrial waste.

For acidified verdete production, 3 g of ground verdete rock was reacted with 12 mL of AIE in 50 mL centrifuge tubes and stirred at 150 rpm on a horizontal shaker table for 72 h. After shaking, the tubes were opened and placed in a water bath at 90 ± 5 °C for 4 h in order to reduce or eliminate excess fluorine. The material was then dried in an air circulation laboratory oven at 105 °C for 72 h. After cooling, this material was ground in an agate mortar and passed through a 150 μm sieve for standardization and stored in acrylic tubes.

2.3 Calcined Verdete

Ground verdete rock and $\text{CaCl}_2 \cdot 2\text{H}_2\text{O}$ were mixed at a 1:1 ratio. Samples of 4 g of this mixture were placed in carbon crucibles and calcined in a muffle furnace at 900 °C for 60 min. The heating ramp was linear with a duration of 45 min. After calcination, the products were crushed in an agate mortar and passed through a sieve with a 150 μm

mesh. Previous calcination test of verdete using the $\text{CaCl}_2 \cdot 2\text{H}_2\text{O}$ as fluxing agent indicated the 900 °C at 60 min was the best treatment to solubilize verdete (*Santos et al.*, 2015)..

2.4 Chemical analysis

Total, water-soluble and citric acid-soluble K from natural rock, acidified and calcined verdete as well as KCl were measured as described by *Alcarde* (2009), in accordance with the Brazilian Ministry of Agriculture, Livestock and Food Supply Normative Instruction #5 (*BRASIL*, 2007). Citric acid is a non-standard extracting solution for K fertilizers, but it was used due to the low water solubility of K in the silicate rock. On the other hand, citric acid is generally produced in high amounts in the rhizosphere.

The total K concentration of samples was analyzed using the tri-acid digestion method EPA 3052 (1996). For water soluble K analysis, samples of 1.0 g of fertilizers were placed in an Erlenmeyer flask with 50 mL of distilled water. Suspensions were then boiled on a hot plate for 10 min. Potassium that was soluble in 2% citric acid was measured by extracting 0.5 g of fertilizer with 50 mL of this solution. Samples were shaken at 150 rpm for 30 min in a horizontal laboratory shaker. Samples from both extractions were filtered using filter Whatman Grade 595 (4 - 7 μm). The K concentration in all extracts was determined in triplicate by flame emission spectrophotometry. The relative abundance of water or citric acid-soluble K (%) was calculated using the total amount of K in each fertilizer.

2.5 X-ray diffraction (XRD)

X-ray diffraction (XRD) analysis of samples before and after each treatment was carried out using an X'Pert Pro MPD Panalytical diffractometer in the 4 to 80° 2θ range with Co-K α radiation ($\lambda = 1.789 \text{ \AA}$), at a rate of 0.02° 2θ s⁻¹, operated at 40 kV and 30 mA. Powder mounts were prepared by packing ground ($\leq 0.075 \text{ mm}$) samples into

aluminum holders. Minerals identification was performed using the *American Mineralogist Crystal Structure Database* (<http://rruff.geo.arizona.edu/AMS/amcsd.php>).

2.6 Greenhouse trials

The agronomic efficiency of fertilizers was evaluated in a greenhouse pot experiment using two separate cropping systems: grass was grown in succession of maize and, eucalyptus was tested in a single cultivation. Soil was collected from the top layer (0-30 cm) of the soil profile and was a red-yellow Oxisol. Samples were air-dried and passed through a sieve (4 mm) for the pot trial experiments and 2 mm for chemical and physical analysis. Soil (3 and 4 dm³) was put into the plastic bags and lime (CaCO₃:MgCO₃ at Ca/Mg ratio of 4:1) was applied aiming the percent base saturation of 60%. Soil was wetted to 80% of the maximum field capacity and maintained at that level for 30 d. After this time, soil was dried, homogenized and re-analyzed. Briefly, the soil had low K concentrations (17 mg dm⁻³, Mehlich-1 extractor) and was comprised 72% clay, with a pH_{H2O} of 5.6, Ca²⁺ and Mg²⁺ concentrations of 18.3 and 4.7 mmolc dm⁻³, respectively (KCl 1 M extractor) and a soil organic C concentration of 15.5 g kg⁻¹ (*Walkley and Black, 1934*). Basal nutrients N, P, S, Zn, Mn, Fe, Cu, B and Mo were applied at rate of (mg dm⁻³) 150, 300, 80, 4, 3.6, 1.5, 1.3, 0.8 and 0.15 mg dm⁻³, respectively. Soil and fertilizers were mixed before repotting.

Treatments were designed in a factorial scheme 4 x 3 + 1, evaluating four K sources (verdete rock; acidified verdete rock; calcined verdete rock and KCl) at three rates of K (50, 100 and 200 mg dm⁻³). A control without K application was included. The experiment was a randomized design with four replications. Forms and rate of K sources were evaluated in three crops (maize-grass succession and eucalyptus).

2.6.1 Maize-Grass succession

Five seeds of maize (*Zea mays* L.) were planted in pots containing 3 dm³ of soil, and two plants grown for 45 d. Roots and shoots were harvested separately and washed with distilled water prior to chemical analysis. Approximately 300 cm³ of soil was collected for chemical analysis. The remaining soil samples (approximately 2.7 dm³) were air dried, homogenized and passed through a sieve with a 4 mm mesh and repotting. Then grass seeds (*Panicum maximum* cv. Mombaça) were sown and cultivated for 60 d in the same soil samples. The same process was performed for the vegetal material and soil sampling as describe above.

2.6.2 Eucalyptus cultivation

For eucalyptus cultivation, seedlings (clone I 144) were grown in 4 dm³ of soil for 90 d. It were used the same treatments and experimental design above described by maize-grass succession. Shoot and roots were again harvested separately. Soil samples (300 cm³) were collected at the end of all experiments analyzed to determine the K concentration.

Vegetal parts were dried in a forced air furnace until constant weight at 65 °C. The material was weighed, milled, and digested using a nitric-perchloric solution (*Johnson and Ulrich, 1959*). Soil samples were air dried and analyzed for Mehlich-1 extractable K (*Nelson et al., 1953*). For all extracts, K concentrations were measured using flame emission spectrophotometry (B462- Micronal).

2.7 Data and statistical analysis

Data was statistically analyzed using ANOVA. The effects of K dose on dry matter, total K content, K content on reference leaves, and soil K availability for each source were determined using regression analysis. The recovery of K was calculated by slope of regression model of K content divided by volume of soil for each cultivation.

3 Results

3.1 Chemical characterization

Verdete rock comprised approximately 9.3% total K_2O ($w w^{-1}$) and had a very low K solubility in water and in 2% citric acid (Table 2). Only 0.6% of the total concentration of K was water-soluble, and only 2.1% was citric acid-soluble. Chemical and thermal treatments increased K solubility in verdete rock and resulted in a mass increase and a consequent dilution of the total K content in the treated products (Table 2). The total concentration of K_2O was 5.3 and 4.3% ($w w^{-1}$) after chemical and thermal treatments of verdete rock, respectively. The extractability of K in water was 81% and 93% for acidified verdete and calcined verdete, respectively. This corresponds to an increase in reactivity of 145- and 167-fold, respectively. Using citric acid, reactivity increased by 27- and 48-fold, while the K extractabilities of acidified and calcinated verdete were 57 and 100% respectively. The extractability of K from acidified verdete was less in citric acid (57%) to compared to than in water (81%) (Table 2).

3.2 Mineralogical characterization

The diffractogram for verdete rock showed K silicate minerals such as glauconite [$K_2(Mg,Fe)_2Al_6(Si_4O_{10})_3(OH)_{12}$], with Bragg peaks (BP) at 0.99, 0.495, 0.33 and 0.257 nm and microcline ($KAlSi_3O_8$), with BP at 0.646, 0.588, 0.379, 0.346, 0.323, 0.300 and 0.290 nm. Quartz (Si_2O) was also observed with BP at 0.425, 0.334, 0.228 and 0.181 nm

(Fig. 1).

After thermal treatment, these crystalline K minerals collapsed and a new phase, sylvite (KCl), was observed through identification of BP at 0.313, 0.222, 0.181 and 0.157 nm. Sylvite is a water-soluble K mineral and was identified on the diffractograms (Fig. 1). After chemical treatment, partial decomposition of crystalline K minerals from verdete rock were observed (Fig. 1). Although less intense, peaks were still observed for glauconite (0.99, 0.495, 0.33 and 0.257 nm) and microcline (0.646, 0.300 and 0.290 nm). Moreover, peaks associated with arcanite (0.416, 0.351, 0.338, 0.299, 0.290, 0.266, 0.251, 0.242, 0.237, 0.220, 0.208, 0.200, 0.189, 0.169 and 0.145 nm) were also detected. Such mineral formation is related to the reaction of K in glauconite or microcline with sulfate present in the AIE (Fig. 1, Table 1).

After thermal and chemical treatments, the only detected mineral was quartz (Fig. 1). It was observed with less intensity, with BP at 0.425, 0.334 and 0.245 nm.

3.3 Greenhouse trials: growth and potassium uptake by crops

Verdete rock did not significantly affect the growth or K uptake by maize and eucalyptus. However, dry matter and K content in grass increased linearly with the rate of K addition. (Table 3 and Fig. 2). The recovery of K from verdete rock by grass was 6.1% of the total amount of K applied (Table 4).

The K uptake and growth of maize were not significantly different ($p \leq 0.05$) between chemical or thermal verdete rock treatments and KCl (Fig. 2). Dry matter production of maize had a quadratic response with rate of K applied as KCl, acidified and calcined verdete and reached maximum values with 200, 165 and 172 mg dm⁻³ of K, respectively. However, the effect of these fertilizers on grass cultivation after maize was distinct. While KCl applied to maize had no significant effect on K uptake for grass, biomass did

increase linearly following the application of calcined verdete. A similar quadratic response was observed for acidified verdete (maximum values with $125 \text{ mg dm}^{-3} \text{ K}$) (Table 3 and Fig. 2). The recoveries of K in maize following growth for 45 d were 70, 78.3 and 74.6% of the total amount of K applied as either acidified or calcined verdete and KCl, respectively (Table 4). Grass growth in maize succession for 60 d increased 2.4, 4.0 and 2.2% the K recovery with application of acidified or calcined verdete and KCl, respectively (Table 4).

Despite the low concentration of K in soil (17 mg dm^{-3}), the application of K had no effect on eucalyptus growth until 90 d after planting (Table 3 and Fig. 2). Similarly, verdete rock did not change the amount of K taken up by plants. However, treated rock and KCl resulted in a linear increase in K content in eucalyptus plants (Fig. 2). Potassium recoveries in eucalyptus that were grown for 90 d were 53, 51.7 and 59.7% of the total amount of K applied as either acidified or calcined verdete and KCl, respectively (Table 4).

The K concentration was below the critical value in reference leave for maize (17.5 g kg^{-1}), grass (10.8 g kg^{-1}) and eucalyptus (10 g kg^{-1}) where K was not applied. It can be verified from the intercept of the regression equations (Table 3). Concentrations of K in the reference leaves increased linearly with increasing fertilizer K application, except in the eucalyptus when applied as verdete rock (no response) and as calcined verdete (quadratic response) (Table 3). Sufficient K in maize leaves was reached following the application of 82, 148, 165 and $155 \text{ mg dm}^{-3} \text{ K}$ as verdete rock, acidified or calcined verdete and KCl, respectively. For eucalyptus, sufficient K in leaves was reached with the application of 275, 125 and $200 \text{ mg dm}^{-3} \text{ K}$ as acidified or calcined verdete and KCl, respectively (Table 3). The reference values for sufficient K in leaves have ranged in

maize from 17.5 to 22.5 g kg⁻¹, in grass from 10.8 to 16.5 g kg⁻¹ and eucalyptus from 10 to 12 g kg⁻¹ (Martinez *et al.*, 1999).

3.4 Potassium in soil

Soil testing after harvest showed low concentrations of K, even in soils that had the highest doses of K fertilizers (Table 3 and Fig. 2). Verdete rock and KCl did not change K concentrations in soil after maize cultivation, whereas application of treated rock caused a linear increase in K concentrations. However, the low values for slopes of the regression equation (0.030 and 0.046) do show a slight increase. Potassium concentrations in soil reached 17 and 20 mg dm⁻³ at an application rate of 200 mg dm⁻³ K, when K was applied as acidified and calcined verdete, respectively (Table 3 and Fig. 2). After the eucalyptus cultivation, the K concentration in soil was still lower than that in maize as verified by the intercept and slope of the regression equation (Table 3 and Fig. 2).

4 Discussion

4.1 Mineralogical and chemical characterization

The high energy at which K is bonded to the structure of silicates, such as glauconite and microcline, result in its low water solubility. This high stability is related to the fact that K occupies interlayer spaces and is strongly bonded to tetrahedral oxygens in mica-type materials, which have predominantly tetrahedral-sheet charge deficiencies (Marshall, 1964; Kerns and Mankin, 1968).

Both calcination and acidification of the verdete were effective at increasing the water and citric acid extractability of K. The K solubility was found to be similar to that of KCl. The diffractograms for the calcined and acidified verdete showed that soluble K minerals such as sylvite (KCl) and arcanite (K₂SO₄) formed during the collapsing of

glaucosite or microcline structures in the verdete rock. The solubility of sylvite and arcanite in water at 20 °C are 330 and 111 g L⁻¹, respectively (Haynes, 2014).

Curiously, the potassium mineral from acidified verdete is more soluble in water than in citric acid (Table 2). The citric acid (H₃C₆H₅O₇·H₂O) is a tribasic acid with three dissociation constants (pKa₁=3.15; pKa₂=4.77 and pKa₃=6.40) (Bruckenstein and Kolthoff, 1959). The low pH of AIE (~0) combined with citric acid (2% w v⁻¹) produced a pH of approximately 2.0. At this pH level, the citric acid remains non-dissociated (Bruckenstein and Kolthoff, 1959). This pH certainly contributed to less solubilization of K from acidified verdete in citric acid extracted samples compared to that in water. Also, due to the presence of fluorine in the AIE can to promote the silicon dissolution, however this phase is stable in low pH. The isoelectric point of silicon is at a pH of 1.7 and 3.5, when its polymerization is optimum (Terry, 1983). This propriety associated with the pH of citric acid solution (~2.0), promote higher stability for its polymers, difficult K releasing from acidified verdete (Terry, 1983).

To increase the solubility of K silicate minerals, such as those present in verdete rock (e.g. glaucosite and microcline) the presence of fluxing agents is critical (Santos *et al.*, 2015). Calcium chloride has been used as an effective fluxing agent for silicates (Mazumder *et al.*, 1993; Nascimento *et al.*, 2004a; Santos *et al.*, 2015). According to Mazumder *et al.* (1993), the calcination of glaucosite using the CaCl₂ produces sylvite and calcium oxide as described in Eq. (1).



Chemical stability of the silicates is determined by a combination of structural factors and properties of the metallic cations present (Terry, 1983). The type of acid and the secondary compounds produced during the acid attack have a great influence on the

dissolution of K minerals. The formation of arcanite in the chemical treatment is supported by the high SO_4^{2-} concentration (791 g L^{-1}) in the IEA (Table 1).

Industrial effluent acid has a very low pH and the high concentration of H^+ is important in order to release K from verdete. *Feigenbaum et al.* (1981), reported that at a $\text{pH} \leq 3$, the exchange of K^+ by H^+ is established in mica structure. *Yadav and Sharma* (1992), showed that HCl was the best leaching agent of K from glauconite in comparison with H_2SO_4 , H_3PO_4 and HNO_3 . They were able to solubilize up to 96% of the total K from glauconitic sandstones with HCl 6 mol L^{-1} at $105 \text{ }^\circ\text{C}$ for 180 min. In addition, the fluorine present in the IEA (109 g L^{-1}) was important for dissolving silicon (*Hekim and Fogler*, 1977).

4.2 Plant tests

Our results show that verdete rock could not provide sufficient amounts of K for maize growth. Furthermore, only 6% of the amount applied was taken up by grass that was grown for 60 d in maize succession. Verdete rock application did not change the concentration of K in soil after 45 d of maize cultivation, but an increase in available K in soil was observed after grass growth (60 d). These results demonstrate that K is released very slowly from verdete rock; suggesting a long-term residual effect on plant-available K in soil.

Thermal and chemical treatment of verdete rock produced fertilizers that were similar to KCl in terms of agronomic performance. These results were expected as these treatments greatly increased the solubility of verdete rock. Potassium solubility is an important agronomical index of fertilizer efficiency, since soluble fertilizers are more readily available to plants as showed for maize and eucalyptus cultivation. However, negatives effects on plant growth may be observed where the dissolution of KCl is fast and as a

result increases soil K levels quickly beyond the optimum range. In this case, a slow-release or a not too high water soluble fertilizer would be advantageous.

Corn plants growing for 45 d absorbed more K than the eucalyptus plants that were grown for 90 d. Our study shows that applying calcined verdete K recovered by maize reached a maximum of 78.3%, plus 4% by grass after maize cultivation. For eucalyptus plants, maximum recovery was 59.7% when applied as KCl. A maize crop takes up high amounts of K to support the initial growth while eucalyptus plants have a low initial requirement. Besides the distinct ability to acquire K from the soil, plants have different abilities to utilize K physiologically (*Samal et al.*, 2010; *Hafsi et al.*, 2011). Our results show that eucalyptus takes up more K with increasing fertilizers doses but not this does not necessarily increase its growth as was seen in maize. The ability of eucalyptus to achieve maximum growth at a lower K supply may be a consequence of its lower physiological K requirements than maize.

Soil concentrations of K did not increase following the addition of KCl to soil. This may be due to the rapid plant uptake of K by maize. Because the K uptake by maize, K in soil did not increase with increasing KCl doses. However, it was verified with treated verdete rock application. The gradual increases in available K in soil with treated verdete rock show that such sources are suitable in crops succession, mainly in those areas with potential for this nutrient to be lost through leaching.

In light of the above, soluble K fertilizers are produced through of calcination or acidification of K silicate rocks. These fertilizers were similar to KCl in terms of agronomic performance. However, the low K concentrations make them uncompetitive compared to conventional K fertilizer (KCl). But price increases of conventional products as observed in 2008/2009 stimulate non-conventional sources for K fertilizers and make them viable for local use. Moreover, our study shows that a potential industrial waste can

be used to increase the rock solubility, thereby producing a low-cost K fertilizer with sulfur.

5 Conclusions

Given the need for K fertilizer production, particularly in regions distant from sources of conventional products, the results presented here demonstrate that thermal and chemical treatments of verdete rock with $\text{CaCl}_2 \cdot 2\text{H}_2\text{O}$ as fluxing agents and IEA respectively, modify its mineral composition from insoluble K minerals to water-soluble K minerals. Such transformations are important for agronomic performance of these fertilizers when compared to conventional sources, like KCl. Verdete rock had no effects on maize and eucalyptus growth. However, in the second cultivation this rock promoted increase in K absorption by grass, indicating its reactivity increasing. Potassium uptake in grass and maize from verdete was equal to 6% of the total amount applied. Thermal and chemical processes are efficient to increase the reactivity of verdete rock and aiming the production of K-soluble fertilizers.

Acknowledgement

The authors are thankful for the financial support received from FAPEMIG (Fundação de Amparo à Pesquisa do Estado de Minas Gerais – APQ-04092-10).

References

- Alcarde, J.* (2009): Manual de análise de fertilizantes. FEALQ, Piracicaba, Brasil p. 259.
- Alecrim, J. D.* (1982): Recursos minerais do Estado de Minas Gerais. METAMIG, Belo Horizonte, Brasil p. 299.
- Bakken, A., Gautneb, H., Sveistrup, T., Myhr, K.* (2000): Crushed rocks and mine tailings applied as K fertilizers on grassland. *Nutr Cycl Agroecosys.* 56, 53-57.
- Blum, W., Herbinger, B., Mentler, A., Ottner, F., Pollak, M., Unger, E., Wenzel, W.* (1989): The use of rock powders in agriculture. 1. Chemical and mineralogical

- composition and suitability of rock powders for fertilization. *Z Pflanz Bodenkunde*. 152, 421-425.
- BRASIL*. (2007): Instrução normativa n. 5, de 23 de fevereiro de 2007. MAPA, Brasília, Brasil.
- BRASIL*. (2011): Resolução n. 430, de maio de 2011. MAPA, Brasília, Brasil.
- Bruckenstein, S., Kolthoff, I.* (1959): Acid-base strength and protolysis curves in water, in *Treatise on analytical chemistry*. Interscience New York, p 462.
- Coroneos, C., Hinsinger, P., Gilkes, R.* (1995): Granite powder as a source of potassium for plants: a glasshouse bioassay comparing two pasture species. *Fert Res*. 45, 143-152.
- da Silva, A. A. S., Medeiros, M. E., Sampaio, J. A., Garrido, F. M. S.* (2012): Caracterização do Verdete de Cedro do Abaeté para o desenvolvimento de um material com liberação controlada de potássio. *HOLOS*. 5, 42-51.
- Eichler, V.* (1983): Disponibilidade do potássio do verdete de Abaeté calcinado com e sem calcário magnesiano, para a cultura do milho em solos de textura média e argilosa. Tese de Doutorado, Universidade Federal de Lavras, Brasil.
- Feigenbaum, S., Edelstein, R., Shainberg, I.* (1981): Release rate of potassium and structural cations from micas to ion exchangers in dilute solutions. *Soil Sci Soc Am J*. 45, 501-506.
- Hafsi, C., Atia, A., Lakhdar, A., Debez, A., Abdelly, C.* (2011): Differential responses in potassium absorption and use efficiencies in the halophytes *Catapodium rigidum* and *Hordeum maritimum* to various potassium concentrations in the medium. *Plant Prod Sci*. 14, 135-140.
- Haynes, W. M.* (2014): *CRC Handbook of chemistry and physics*. CRC press, Florida, USA. p. 2704.

- Hekim, Y., Fogler, H. S. (1977): Acidization—VI: on the equilibrium relationships and stoichiometry of reactions in mud acid. Chem Eng Sci. 32, 1-9.*
- Johnson, C. M., Ulrich, A. (1959): Analytical methods for use in plant analysis. University of California, California, USA p. 54.*
- Kerns, R., Mankin, C. (1968): Structural charge site influence on the interlayer hydration of expandable three-sheet clay minerals. Clays Clay Miner. 16, 73-81.*
- Lima, T. M., Neves, C. A. R. (2012): Sumário Mineral 2012. DNPM, Brasília.*
- Loureiro, F. L., Nascimento, M., Neumann, R., Rizzo, A. C. (2010): Tecnologias de aplicação de glauconita como fonte de potássio na agricultura: o caso brasileiro e a experiência indiana. Anais do I Congresso Brasileiro de Rochagem. 1, 111-119.*
- Madaras, M., Mayerová, M., Kulhánek, M., Koubová, M., Faltus, M. (2013): Waste silicate minerals as potassium sources: a greenhouse study on spring barley. Arch Agron Soil Sci. 59, 671-683.*
- Marshall, C. E. (1964): Physical chemistry and mineralogy of soils, John Wiley & Sons, New York, USA p. 388.*
- Martinez, H., Carvalho, J., Souza, R. (1999): Diagnose foliar, in Ribeiro A, Guimarães P, Alvarez V VH.: Recomendações para uso de corretivos e fertilizantes em Minas Gerais. 5a Aproximação. Sociedade Brasileira de Ciência do Solo, Viçosa, Brasil.,pp. 143-167.*
- Mazumder, A., Sharma, T., Rao, T. (1993): Extraction of potassium from glauconitic sandstone by the roast-leach method. Int J Miner Process. 38, 111-123.*
- Mohammed, S., Brandt, K., Gray, N., White, M., Manning, D. (2014): Comparison of silicate minerals as sources of potassium for plant nutrition in sandy soil. Eur J Soil Sci. 65, 653-662.*

- Nascimento, M.* (2004a): Desenvolvimento de método para extração de potássio a partir de feldspato potássico. Tese de Doutorado, Universidade Federal do Rio de Janeiro, Brasil.
- Nascimento, M.* (2004b): Fertilizantes e sustentabilidade: o potássio na agricultura brasileira, fontes e rotas alternativas. CETEM/MCT, p. 61.
- Nelson, W., Mehlich, A., Winters, E.* (1953): The development, evaluation, and use of soil tests for phosphorus availability. *Agronomy*. 4, 153-188.
- Ott, H.* (2012): Fertilizer markets and their interplay with commodity and food prices. *JRC Scientific and Policy Reports*, 1-34.
- Ramezani, A., Dahlin, AS., Campbell, CD., Hillier, S., Mannerstedt-Fogelfors, B., Öborn, I.* (2013): Addition of a volcanic rockdust to soils has no observable effects on plant yield and nutrient status or on soil microbial activity. *Plant Soil*. 367, 419-436.
- Samal, D., Kovar, J. L., Steingrobe, B., Sadana, U. S., Bhadoria, P. S., Claassen, N.* (2010): Potassium uptake efficiency and dynamics in the rhizosphere of maize (*Zea mays* L.), wheat (*Triticum aestivum* L.), and sugar beet (*Beta vulgaris* L.) evaluated with a mechanistic model. *Plant Soil*. 332, 105-121.
- Santos, W. O., Mattiello, E. M., Costa, L. M., Abrahão, W. A. P., Novais, R. F., Cantarutti, R. B.* (2015): Thermal and chemical solubilization of verdete for use as potassium fertilizer. *Int J Miner Process*. 140, 72-78.
- Terry, B.* (1983): The acid decomposition of silicate minerals Part I. Reactivities and modes of dissolution of silicates. *Hydrometallurgy*. 10, 135-150.
- Toledo Piza, P. A., Bertolino, L. C., Silva, A. A. S., Sampaio, J. A., Luz, A. B.* (2011): Verdete da região de Cedro de Abaeté (MG) como fonte alternativa para potássio. *Geociências*. 30, 345-356.

Valarelli, J. V., Novais, R. F., Vaz, M. M. T. (1993): Ardósias" Verdete" de Cedro do Abaeté na Produção de Termofosfato Potássico Fundido e sua Eficiência Agronômica. *An Acad Bras Ciências*. 65, 363-376.

Varadachari, C. (1992): An investigation on the reaction of phosphoric acid with mica at elevated temperatures. *Ind Eng Chem Res*. 31, 357-364.

Walkley, A., Black, I. A. (1934): An examination of the Degtjareff method for determining soil organic matter, and a proposed modification of the chromic acid titration method. *Soil Sci*. 37, 29-38.

Yadav, V., Sharma, T. (1992): Leaching of glauconitic sand stone in acid lixivants. *Miner Eng*. 5, 715-720.

Table 1: Chemical characteristics of the industrial effluent acid (IEA) from London & Scandinavian Metallurgical_ Brazil S.A

pH	Ca	Mg	K	Fe	Zn	Cu	Mn	Al
-----mg L ⁻¹ -----								
0.0	46	4.7	3438	13595	44	57	1199	897
Cr	Ni	Pb	F ⁻	SO ₄ ²⁻	NO ₃ ⁻	PO ₄ ³⁻	Cl ⁻	
-----mg L ⁻¹ -----			-----g L ⁻¹ -----					
59	126	56	109	791	18	19	128	

Cl⁻, F⁻, SO₄²⁻, NO₃⁻, PO₄³⁻ contents were determined by liquid ionic chromatography (DX500, Dionex-Sunnyvale-CA), according Silva et al. (2001). Cd, Ni, Pb, Cd, Cr, Al, Fe, Mn, Cu, Zn, Ca e Mg contents were determined by optic spectroscopy plasma emission (ICP-OES) (PerkinElmer, Optima TM 4300DV). K content was determined by flame emission spectrophotometry (B462- Micronal).

Table 2: Total, water and citric acid soluble K₂O content in verdete rock, acidified and calcined verdete and KCl

Product	Total K ₂ O	Soluble K (% w w ⁻¹ total K)	
		water	citric acid
		-----%-----	
Verdete rock	9.33±0.20	0.56±0.45	2.10±0.15
Acidified Verdete	5.32±0.18	80.62±3.7	57.31±2.1
Calcined Verdete	4.30±0.13	93.66±3.0	100.00±1.3
KCl	52.1±0.09	100.00±0.1	100.00±0.0

Table 3: Regression equations that describe the effect of forms and rates of potassium fertilizers on dry matter production, K uptake and concentration in leaves of maize, grass in maize succession and eucalyptus and K in soil at the end of each growing period

Product	Maize		Grass		Eucalyptus	
	Regression equation	R ²	Regression equation	R ²	Regression equation	R ²
	-----Dry matter (g pot ⁻¹)-----					
Verdete rock	$\hat{y}=\bar{y}=25.03$	-	$\hat{y}=2.52+0.006^{**}x$	0.99	$\hat{y}=\bar{y}=187.54$	-
Acidified verdete	$\hat{y}=23.24+0.264^{**}x-0.0008^{***}x^2$	0.99	$\hat{y}=2.60+0.01^0x-0.00004^0x^2$	0.85	$\hat{y}=\bar{y}=203.35$	-
Calcined verdete	$\hat{y}=23.50+0.241^{**}x-0.0007^{***}x^2$	0.98	$\hat{y}=2.41+0.003^0x$	0.70	$\hat{y}=\bar{y}=194.49$	-
KCl	$\hat{y}=23.91+0.200^{**}x-0.0005^{***}x^2$	0.94	$\hat{y}=\bar{y}=2.76$	-	$\hat{y}=\bar{y}=202.06$	-
	-----K uptake (mg pot ⁻¹)-----					
Verdete rock	$\hat{y}=\bar{y}=127.34$	-	$\hat{y}=17.47+0.166^{***}x$	0.99	$\hat{y}=\bar{y}=409.43$	-
Acidified verdete	$\hat{y}=155.98+2.097^{***}x$	0.97	$\hat{y}=19.45+0.066^{**}x$	0.76	$\hat{y}=365.5+2.12^{***}x$	0.95
Calcined verdete	$\hat{y}=141.81+2.351^{***}x$	0.98	$\hat{y}=16.06+0.108^{***}x$	0.99	$\hat{y}=433.0+2.07^{***}x$	0.94
KCl	$\hat{y}=145.72+2.238^{***}x$	0.97	$\hat{y}=19.18+0.06^{**}x$	0.76	$\hat{y}=367.3+2.39^{***}x$	0.97
	-----K concentration in reference leaves (g kg ⁻¹)-----					
Verdete rock	$\hat{y}=13.45+0.05^{***}x$	0.63	$\hat{y}=12.42+0.037^{***}x$	0.97	$\hat{y}=\bar{y}=6.29$	-
Acidified verdete	$\hat{y}=11.65+0.040^{***}x$	0.78	$\hat{y}=11.77+0.015^{**}x$	0.97	$\hat{y}=5.36+0.017^{**}x$	0.71
Calcined verdete	$\hat{y}=11.94+0.034^{***}x$	0.80	$\hat{y}=12.124+0.032^{***}x$	0.99	$\hat{y}=6.46+0.050^{**}x-0.0002^{**}x^2$	0.94
KCl	$\hat{y}=11.69+0.038^{***}x$	0.86	$\hat{y}=12.35+0.017^{**}x$	0.93	$\hat{y}=6.01+0.020^{**}x$	0.93
	-----K in soil (mg dm ⁻³)-----					
Verdete rock	$\hat{y}=\bar{y}=12.98$	-	$\hat{y}=6.69+0.007^{**}x$	0.91	$\hat{y}=5.69+0.089^{***}x-0.0004^{**}x^2$	0.89
Acidified verdete	$\hat{y}=11.68+0.030^{**}x$	0.94	$\hat{y}=6.36+0.004^0x$	0.59	$\hat{y}=5.31+0.020^{**}x$	0.97
Calcined verdete	$\hat{y}=10.85+0.046^{***}x$	0.87	$\hat{y}=6.78+0.016^{***}x$	0.97	$\hat{y}=5.83+0.052^{***}x$	0.99
KCl	$\hat{y}=\bar{y}=13.65$	-	$\hat{y}=6.55+0.005^{**}x$	0.71	$\hat{y}=5.65+0.019^{**}x$	0.90

0, *, **, ***, significant at 10, 5, 1 and 0.1% of probability by the *t* test.

Table 4: Estimated values of potassium uptake and their respective recoveries by crops with different forms and rates of potassium fertilizers in an Oxisol with native 17 mg dm⁻³ of K (Mehlich-1)

Product	K applied	K uptake				K recovered			
		Maize	Grass	Maize + Grass	Eucalyptus	Maize	Grass	Maize + Grass	Eucalyptus
		-----mg dm ⁻³ -----				----- % of amount applied-----			
Verdete rock	0		6.5	48.9					
	50		9.5	51.9					
	100	42.4	12.6	55.0	102.4	-	6.1	6.1	-
	200		18.8	61.2					
Acidified verdete	0	52.0	7.2	59.2	91.4				
	50	86.9	8.4	95.4	117.9				
	100	121.9	9.6	131.5	144.4	70.0	2.4	72.4	53.0
	200	191.8	12.1	203.9	197.4				
Calcined verdete	0	47.3	5.9	53.2	108.3				
	50	86.5	7.9	94.4	134.1				
	100	125.6	9.9	135.6	160.0	78.3	4.0	82.3	51.7
	200	204.0	13.9	218.0	211.8				
KCl	0	48.6	7.1	55.7	91.8				
	50	85.9	8.2	94.1	121.7				
	100	123.2	9.3	132.5	151.6	74.6	2.2	76.8	59.7
	200	197.8	11.5	209.3	211.3				

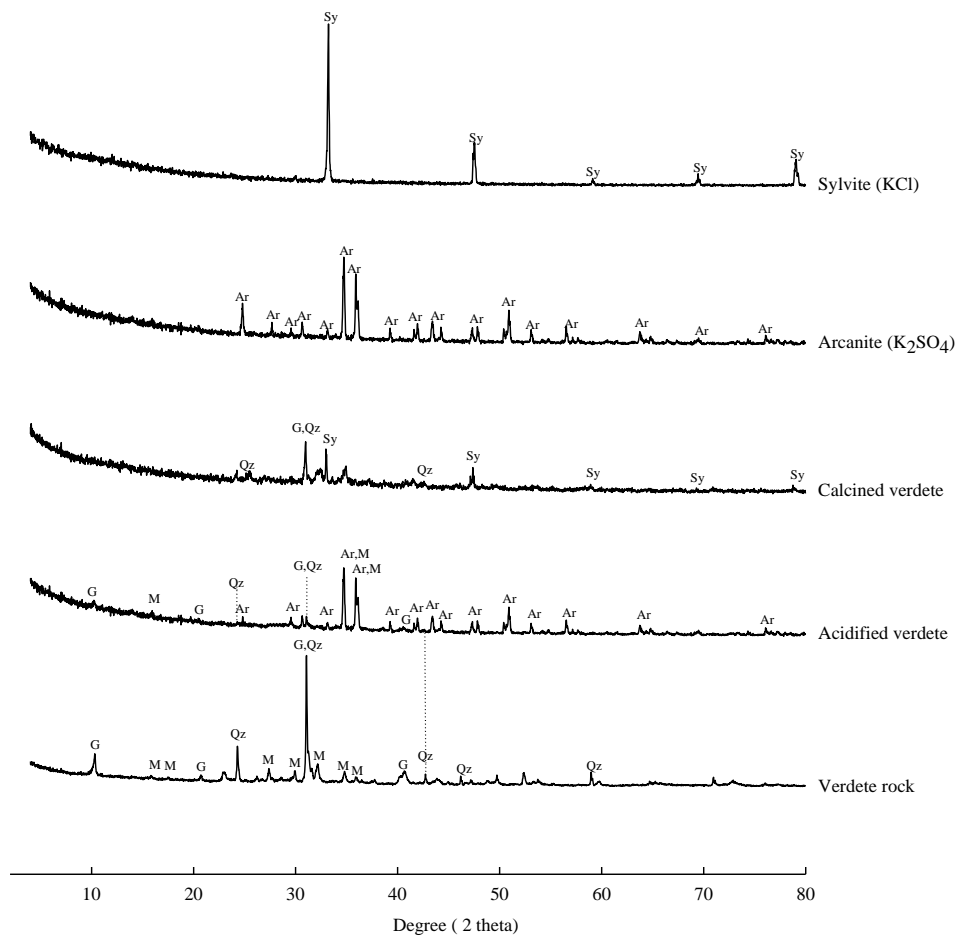


Figure 1: Mineralogical characterization of verdete rock, calcined and acidified verdete and reference samples of sylvite (KCl) and arcanite (K₂SO₄). Co K_α radiation (1.789 Å). QZ: quartz (SiO₂); G: glauconite [K₂(Mg,Fe)₂Al₆(Si₄O₁₀)₃(OH)₁₂]; Sy: sylvite (KCl); Ar: arcanite (K₂SO₄) and M: microcline (KAlSi₃O₈).

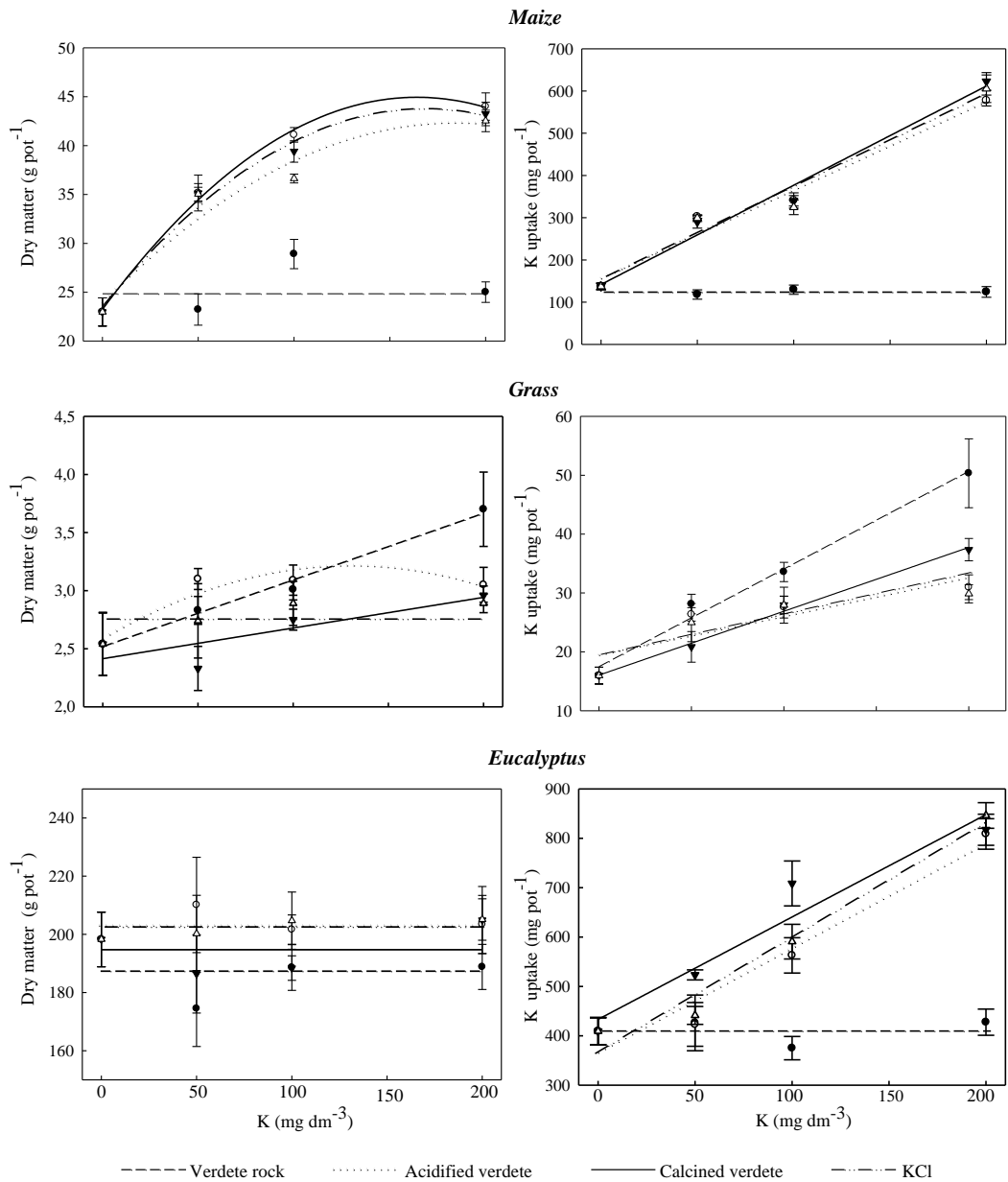


Figure 2: Regression graphics that describe the effect of forms and rates of potassium fertilizers on dry matter production and K uptake in maize, grass in maize succession and eucalyptus. Cross-bar (I) represents the standard error with 4 replications.

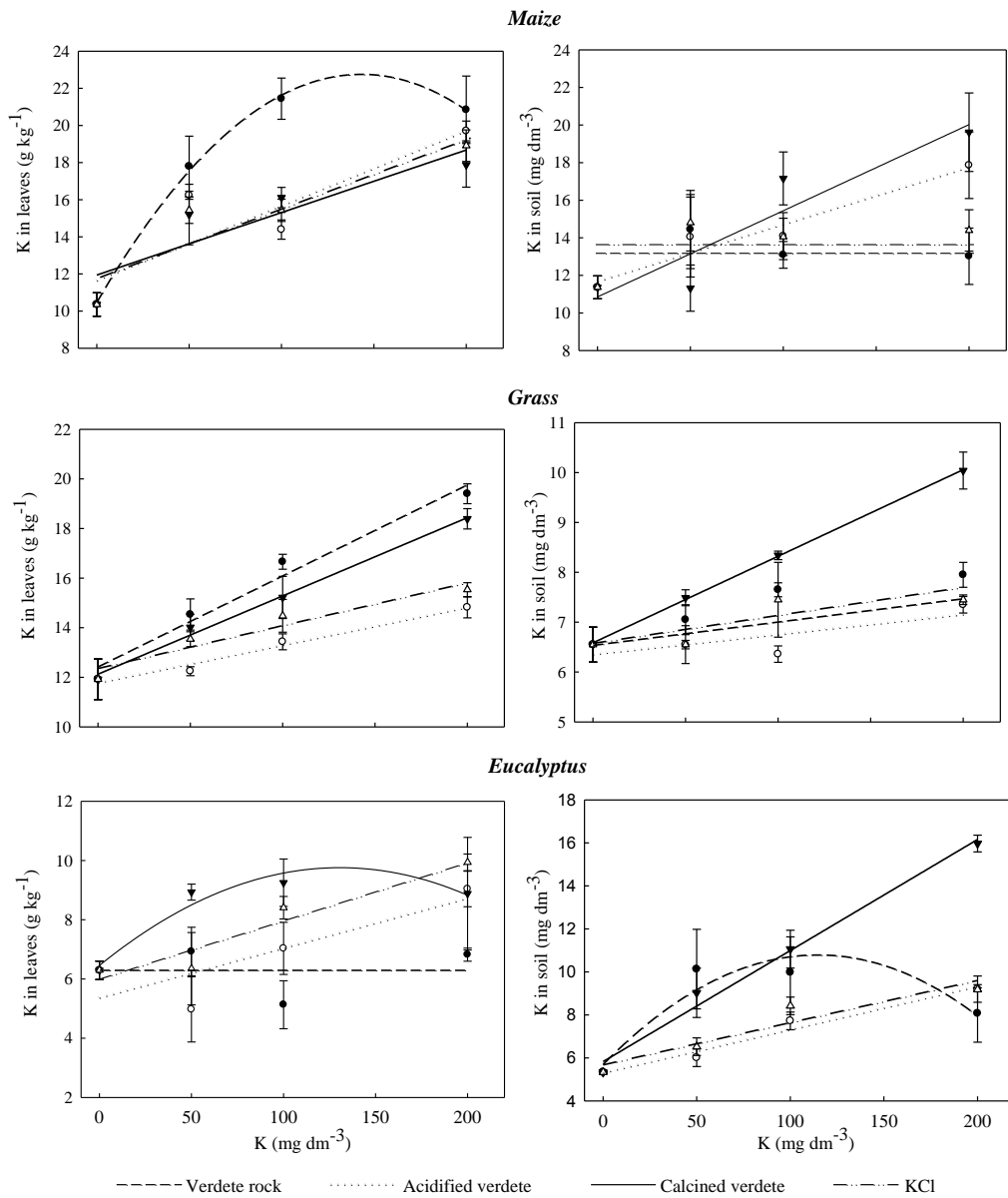


Figure 3: Regression graphics that describe the effect of forms and rates of potassium fertilizers on K concentration in leaves of maize, grass and eucalyptus and in soil. Cross-bar (I) represents the standard error with 4 replications.

CONCLUSÕES GERAIS

A calcinação do verdete mostrou-se ser uma técnica eficaz para a solubilização da rocha, sendo que na presença do agente fundente $\text{CaCl}_2 \cdot 2\text{H}_2\text{O}$ foi possível obter até 96% do K total solúvel em água. A formação de sylvita (KCl) com a calcinação da rocha foi confirmada, entretanto a análise Potassium K-edge XANES indicou que, além do KCl, desconhecidas fases potássicas solúveis também se formaram. Esse indicativo abre novas perspectivas de estudos objetivando a identificação e separação dessas espécies para agregar maior valor ao produto.

O uso de efluente ácido proveniente da metalurgia do Ta e Nb foi capaz de solubilizar parcialmente a rocha verdete, possibilitando a extração de cerca de 81% do K total em água. O mineral arcanita (K_2SO_4) foi formado devido a esse processo. Assim, o produto desse processo além de fonte de K, representa também uma fonte de S. Experimento em casa de vegetação comprovaram que tanto o produto da calcinação, quando da acidificação do verdete, possuem eficiências agrônômicas equivalentes ao KCl nos cultivos de milho e eucalipto. Por outro lado, a aplicação do verdete moído *in natura* não teve efeito nos cultivos de milho e eucalipto, porém demonstrou efeito residual para o capim cultivado em sucessão ao milho.

O mesmo efluente ácido utilizado na solubilização do verdete foi eficaz na solubilização dos fosfatos de Araxá, Patos e Bayóvar, aumentando expressivamente os teores de P extraíveis em água, citrato neutro de amônio ou ácido cítrico. Análises de difração de raios X, associada com Phosphorus K-edge XANES mostram que aumentando a concentração do efluente, fosfatos tricálcicos (apatitas) são gradativamente dissolvidas e convertidas em fases mais solúveis de P, como fosfatos tricálcicos amorfos, fosfatos dicálcicos, fosfatos monocálcicos e fosfatos de ferro (III) amorfos. Análise na pré-borda do P (~2148 eV), mostra que a formação de fosfatos de ferro (III) é progressiva com o aumento da concentração do efluente. A suavização na pós-borda (~2155 eV), com o aumento da concentração do efluente, confirmou a formação de espécies de P menos rica em Ca.

O desenvolvimento dessa tese abre novas perspectivas no aproveitamento de rochas silicatadas para a produção de fertilizante potássico, seja por meio de tratamento térmico, como utilizando efluente ácido. Adicionalmente, informa que, utilizando o efluente ácido, é possível obter fertilizantes fosfatados com reatividade aumentada, a partir de fosfatos naturais oriundos de depósitos sedimentares, ígneos ou metamórficos. Entretanto, estudos com plantas são necessários para a comprovação da eficácia desses produtos como fertilizantes.